

Morphology of fans in the high-arctic periglacial environment of Svalbard: controls and processes

Tjalling de Haas^a, Maarten G. Kleinhans^a, Patrice E. Carbonneau^b, Lena Rubensdotter^{c,d}, Ernst Hauber^e

^a*Faculty of Geosciences, Utrecht University, PO-Box 80115, 3508 TC Utrecht, The Netherlands*

^b*Department of Geography, Durham University, DH1 3LE, Durham, UK*

^c*Department of Arctic Geology, University Centre in Svalbard, Longyearbyen, Norway*

^d*Geological Survey of Norway, Trondheim, Norway*

^e*Institute of Planetary Research, German Aerospace Center, Rutherfordstrasse 2, DE-12489 Berlin, Germany*

Abstract

Fan-shaped landforms occur in all climatic regions on Earth. They have been extensively studied in many of these regions, but there are few studies on fans in periglacial, arctic and antarctic regions. Fans in such regions are exposed to many site-specific environmental conditions in addition to their geological and topographic setting: there can be continuous to discontinuous permafrost and snow avalanches and freeze-thaw cycles can be frequent. We study fans in the high-arctic environment of Svalbard to (1) increase our fundamental knowledge on the morphology and morphometry of fans in periglacial environments, and (2) to identify the specific influence of periglacial conditions on fans in these environments. Snow avalanches have a large geomorphic effect on fans on Svalbard: the morphology of colluvial fans is mainly determined by frequent snow avalanches (e.g., flattened cross-profiles, exposed fine-grained talus on the proximal fan domain, debris horns and tails). As a result, there are only few fans with a rockfall-dominated morphology, in contrast to most other regions on Earth. Slush avalanches contribute significant amounts of sediment to the studied alluvial fans. The inactive surfaces of many alluvial fans are rapidly bevelled and levelled by snow avalanches, solifluction and frost weathering. Additionally, periglacial reworking of the fan surface often modifies the original morphology of inactive fan surfaces, for example by the formation of ice-wedge polygons and hummocks. Permafrost lowers the precipitation threshold for debris-flow initiation, but limits debris-flow volumes. Global warming-induced permafrost degradation will likely increase debris-flow activity and -magnitude on fans in periglacial environments. Geomorphic activity on snow avalanche-dominated colluvial fans will probably increase due to future increases in precipitation, but depends locally on climate-induced changes in dominant wind direction.

Keywords: alluvial fan, colluvial fan, periglacial, snow avalanche, debris flow, Svalbard;

Email address: t.dehaas@uu.nl (Tjalling de Haas)

1. Introduction

Fan-shaped deposits are conical landforms that commonly develop where a channel emerges from a mountainous catchment to an adjoining valley (Blair and McPherson, 2009). Fans can vary greatly in size and can be roughly divided into (1) colluvial fans (10s to 100s m), including talus cones and scree slopes (e.g., Blikra and Nemeč, 1998), (2) alluvial fans (100s m to 10s km), generally dominated by sediment-gravity flows or fluid-gravity flows (e.g., Blair and McPherson, 2009) and (3) fluvial fans or megafans (>10s km) (Hartley et al., 2010; Weissmann et al., 2010). These landforms have been described in many environments on Earth (e.g., Blair and McPherson, 2009; Harvey, 2011), Mars (e.g., De Haas et al., 2013; Hauber et al., 2013) and Titan (e.g., Lorenz et al., 2008). Terrestrial regions wherein fans have are present include arid to semi-arid regions (e.g., Whipple and Dunne, 1992; Al-Farraġ and Harvey, 2000; Hartley et al., 2005), humid temperate regions (e.g., Moscariello et al., 2002; Saito and Oguchi, 2005; Chiverrell et al., 2007), alpine environments (e.g., Kostaschuk et al., 1986; Derbyshire and Owen, 1990; Cavalli et al., 2008), the humid tropics (e.g., Kessel and Spicer, 1985) and periglacial, arctic and antarctic environments (hereafter termed ‘periglacial’) (e.g., Catto, 1993; Webb and Fielding, 1999; Davies et al., 2003). While especially fans in arid to semi-arid, alpine and temperate environments have been extensively studied, fans in periglacial environments have received little attention.

The influence of climate on fan formation has long been under debate; some authors believe that changes in climate will be preserved as differences in fan facies and morphology (e.g., Nemeč and Postma, 1993; Dorn, 1994; Ritter et al., 1995), whereas others suggest that climate is rarely the main factor governing fan characteristics (e.g., Blair and McPherson, 1994, 2009). Many different studies suggest that processes leading to fan deposits differ little between humid and arid environments, or between arctic and subtropical environments (e.g., Brierley et al., 1993; Ibbeken et al., 1998; Krzyszkowski and Zieliński, 2002; Harvey et al., 2005; Lafortune et al., 2006), and accordingly fans and debris flows in periglacial regions were found to be not significantly distinct from those in other climates (Catto, 1993; Harris and Gustafson, 1993; Webb and Fielding, 1999). However, fans in periglacial environments are subject to different environmental conditions compared to fans in other climate zones; there can be continuous or discontinuous permafrost, precipitation occurs generally dominantly as snow, snow avalanches can be frequent in mountainous regions and freeze-thaw cycles occur regularly leading to pervasive weathering (e.g., Matsuoka, 1991; Eckerstorfer and Christiansen, 2011b,a). As temperatures are below the freezing point for the largest part of the year, most geomorphic activity is typically limited to a narrow window in the spring and summer months when snow and ice are able to melt and precipitation is able to occur as rain. Recently deglaciated periglacial environments expose landscapes that are in an unstable state, and consequently liable to rapid modification, erosion and sediment release at rates greatly exceeding background denudation rates (e.g., Eyles and Kocsis, 1988; Brazier et al., 1988; Ballantyne, 2002; Mercier et al., 2009). Such accelerated geomorphic activity after deglaciation is termed ‘paraglacial’ (e.g., Ryder, 1971; Ballantyne, 2002). These different controls raise the question to what degree fan formation, deposits and morphology in periglacial environments differ from those in other environments. This is

43 largely unknown due to the small number of studies on periglacial fans (Legget et al., 1966;
44 Catto, 1993; Harris and McDermid, 1998; Webb and Fielding, 1999), illustrating the need
45 for detailed descriptions of fans in these environments.

46 The ongoing global atmospheric warming especially affects the polar and periglacial
47 regions (e.g., Christiansen et al., 2010; Førland et al., 2012). Mainly, it leads to extensive
48 glacier and permafrost degradation (e.g., Benestad, 2005; Etzelmüller et al., 2011), thereby
49 increasing slope activity and hazard potential (e.g., Harris et al., 2011). As fluvial- and
50 alluvial fans are preferred sites for settlements (e.g., Cavalli et al., 2008), this emphasizes
51 the need for a detailed understanding of fans in periglacial environments. For example,
52 catastrophic slope processes, including debris flows and snow avalanches, claimed numerous
53 lives and had considerable economic effects during the last century in periglacial regions such
54 as Iceland, Norway and Svalbard (Jahn, 1967; Jóhannesson and Arnalds, 2001; Decaulne and
55 Sæmundsson, 2003, 2007; Nesje et al., 2007).

56 Here we aim to (1) increase our fundamental knowledge on the morphology and mor-
57 phometry of fans in periglacial environments and to (2) identify the influence of periglacial
58 conditions, such as snow avalanches and continuous permafrost, on fan formation, morphol-
59 ogy and morphometry, by studying colluvial and alluvial fans on Svalbard.

60 In addition to a literature review on slope processes in the periglacial environment of
61 Svalbard, which are responsible for the transport to and redistribution of sediment on fans,
62 a large number of colluvial and alluvial fans were studied in the Adventdalen region on
63 the island of Spitsbergen, in vicinity of Svalbard's capital Longyearbyen (Fig. 1; Table 1;
64 Fig. S1-S6). This region was chosen for its high-arctic location and excellent field research
65 infrastructure including availability of high-resolution imagery and topographic data. More-
66 over, there have been numerous studies on slope processes on Svalbard (e.g., Rapp, 1960;
67 Jahn, 1967; Bibus, 1975; Larsson, 1982; Åkerman, 1984; André, 1990; Siewert et al., 2012;
68 Eckerstorfer et al., 2013), enabling detailed understanding of the processes involved in fan
69 formation.

70 This paper is organized as follows. First, data and methods are described. Next, a
71 detailed summary of the climate, geology and geomorphic slope processes on Svalbard is
72 given, as these factors together are responsible for the formation and characteristics of the
73 fans. Then, the morphology and morphometry of the studied fans in the Adventdalen region
74 are described, in order to identify characteristics that can be unique for fans in periglacial
75 environments. Finally, the specific characteristics that differentiate periglacial fans from
76 those in other environments are discussed, followed by a brief discussion on the effect of
77 present global warming and associated natural hazards on fans in periglacial environments.

78 2. Data and methods

79 This study is based on a combination of high-resolution imagery and geomorphological
80 fieldwork. High-resolution imagery was acquired during a flight campaign in the summer of
81 2008 with the airborne High Resolution Stereo Camera (HRSC-AX) (Gwinner et al., 2000;
82 Neukum and the HRSC-Team, 2001) and a flight campaign in the summer of 2009 with an
83 unmanned airborne vehicle (UAV) carrying a Pentax Optio A4 camera.

Table 1: Geomorphic data of the studied alluvial fans. Fan type abbreviations: AF = cone-shaped snow avalanche-dominated colluvial fan, AFt = tongue-shaped snow avalanche-dominated colluvial fan, DF = debris-flow-dominated fan, FF = fluvial-flow-dominated fan. Note that these abbreviations are based on the processes that dominate the morphology of the fans, and do not necessarily refer to the dominant mechanism of aggradation (some of the colluvial fans have a snow avalanche-dominated surface but might have been mainly aggraded by rock falls). Apex coordinates in UTM WGS84 33N. See supplementary materials for orthophotos of all the fans shown in this table.

No	Valley	Fan type	Apex X	Apex Y	Catchment area, m ²	Catchment relief, m	Catchment length, m	Catchment slope, °	Fan area, m ²	fan relief, m	fan length, m	fan slope, °
1	Longycardalen	AFt	512423	8680605	16098	172	223	38	17621	149	266	29
2	Longycardalen	AF	512496	8680678	16469	162	210	38	22165	165	263	32
3	Longycardalen	AF	512939	8681249	29512	235	268	41	15354	110	232	25
4	Longycardalen	AF	512991	8681393	37922	230	280	39	20407	122	221	29
5	Longycardalen	AF	513024	8681498	22008	225	264	40	12026	128	228	29
6	Longycardalen	AF	513056	8681591	27333	226	277	39	16719	132	242	29
7	Longycardalen	AF	513095	8681672	28800	230	296	38	17465	126	241	28
8	Longycardalen	AF	513131	8681758	22213	221	271	39	20512	140	280	27
9	Longycardalen	AF	513185	8681867	21026	225	288	38	14038	126	246	27
10	Longycardalen	AF	513215	8681954	28646	203	259	38	17036	135	255	28
11	Longycardalen	AF	513254	8682029	17953	198	259	37	15013	173	299	30
12	Longycardalen	AF	513313	8682097	28562	207	274	37	16414	156	286	29
13	Longycardalen	AF	513768	8680667	18913	174	188	43	18250	155	335	25
14	Longycardalen	AF	513789	8680780	23617	206	241	40	25744	139	336	23
15	Longycardalen	AF	513856	8680905	29478	205	252	39	21757	139	311	24
16	Longycardalen	AF	513922	8680987	18850	194	233	40	25526	161	378	23
17	Longycardalen	AF	513926	8681064	15292	214	260	39	21806	135	301	24
18	Hanaskogdalen	DF	515638	8690657	230571	357	867	22	73043	75	420	10
19	Hanaskogdalen	DF	516130	8690708	356622	522	1074	26	198763	101	597	10
20	Hanaskogdalen	DF	516374	8690662	139670	501	915	29	123802	97	519	11
21	Hanaskogdalen	DF	516695	8690688	172311	620	999	32	167826	113	571	11
22	Hanaskogdalen	DF	517326	8690662	250361	606	1124	28	341782	110	727	9
23	Hanaskogdalen	DF	517999	8690788	335505	477	1076	24	184029	93	527	10
24	Hanaskogdalen	DF	518329	8690854	193885	446	1035	23	78200	76	464	9
25	Hanaskogdalen	DF	518561	8690930	370714	555	1207	25	137003	80	487	9
26	Hanaskogdalen	DF	519013	8691190	283326	588	1128	28	270715	98	595	9
27	Hanaskogdalen	DF	519579	8691578	279051	626	1157	28	269162	115	579	11
28	Hanaskogdalen	DF	520070	8691806	307707	555	1182	25	215805	87	544	9
29	Hanaskogdalen	DF	520311	8691885	231832	513	1246	22	92487	67	434	9
30	Mälardalen	DF	519264	8685816	275167	511	1024	27	222839	87	462	11
31	Mälardalen	DF	519639	8686280	226492	516	938	29	246719	96	513	11
32	Mälardalen	AFt	520569	8685626	-	-	-	-	60410	127	463	15
33	Adventdalen	FF	516744	8686209	2254686	830	2355	19	403853	80	619	7
34	Adventdalen	DF	517599	8685897	869820	784	1776	24	231037	108	696	9
35	Adventdalen	DF	518268	8685449	435373	555	1372	22	210850	96	661	8
36	Adventdalen	DF	521910	8681768	-	-	-	-	21757	23	172	8
37	Adventdalen	DF	522142	8681598	-	-	-	-	63640	41	306	8
38	Adventdalen	FF	522693	8681222	-	-	-	-	77040	48	301	9
39	Adventdalen	FF	523250	8680851	749548	804	1934	23	106164	42	257	9
40	Adventdalen	DF	523716	8680690	220045	576	1360	23	125966	66	483	8
41	Bjørndalen	AF	506941	8681423	15831	150	192	38	19060	146	222	33
42	Bjørndalen	AF	506948	8681527	7833	147	178	40	11366	158	233	34
43	Bjørndalen	AF	506959	8681588	12104	161	197	39	16569	157	243	33
44	Bjørndalen	AF	506955	8681675	19851	165	217	37	26098	161	260	32
45	Bjørndalen	AF	506945	8681768	16572	172	222	38	15941	161	259	32
46	Bjørndalen	AF	506936	8681860	18576	179	231	38	20656	162	289	29
47	Bjørndalen	AF	506940	8681949	20045	190	248	38	26156	150	261	30
48	Bjørndalen	AF	506888	8682067	17737	166	209	38	23045	176	272	33
49	Bjørndalen	AF	506839	8682196	23636	159	196	39	29270	183	290	32
50	Bjørndalen	AF	506795	8682365	20518	170	214	38	27415	169	281	31
51	Bjørndalen	AF	506767	8682436	7489	148	163	42	12946	157	242	33
52	Bjørndalen	AF	506732	8682509	28425	172	235	36	28807	172	304	29
53	Bjørndalen	AFt	506643	8680132	16805	183	291	32	14151	97	228	23
54	Bjørndalen	DF	506899	8681200	194619	247	930	15	59915	117	334	19
55	Bjørndalen	FF	508166	8682505	1467265	295	2239	8	165526	147	673	12
56	Bjørndalen	FF	508081	8682022	1520048	369	2808	7	246883	81	612	8
57	Bjørndalen	FF	508034	8681459	591600	305	1832	9	126142	97	494	11
58	Bjørndalen	FF	507939	8681036	637795	344	1809	11	133935	88	488	10
59	Bjørndalen	FF	507689	8680637	834094	325	1709	11	178898	61	543	6
60	Bjørndalen	FF	507449	8680089	612757	383	1642	13	151291	74	481	9
61	Bjørndalen	FF	507209	8679662	297860	323	1558	12	102553	61	417	8
62	Bjørndalen	FF	507113	8679433	344199	367	1629	13	119680	60	415	8

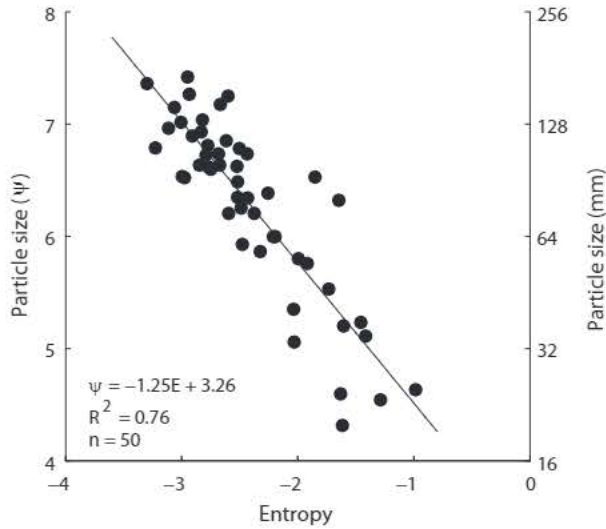


Figure 2: Empirical relation between image entropy in the HRSC-AX image and arithmetic median particle size derived from photosieving. Locations were matched by DGPS and context images.

84 The HRSC-AX is a digital pushbroom (linear array charge-coupled device [CCD]) scanner
 85 with nine channels for nadir panchromatic, stereo panchromatic and color imaging, similar
 86 to its planetary counterpart HRSC on the *Mars Express* (Jaumann et al., 2007). The
 87 images cover $\sim 450 \text{ km}^2$ in the Adventdalen region, large parts of Adventdalen, Bjørndalen,
 88 Longyeardalen, Hanaskogdalen and Mälardalen (Fig. 1c). The processed color and panchro-
 89 matic nadir ortho-images have a spatial resolution (i.e., ground sampling distance) of 20
 90 cm, whilst the digital elevation models (DEMs) derived from stereo images have a spatial
 91 resolution of 50 cm.

92 The UAV images were acquired by Kolibri Geo Services. In total 165 images were shot
 93 covering multiple fan systems in Adventdalen, which we processed with Agisoft Photoscan
 94 software (Agisoft, 2011) into a georeferenced orthorectified image with a spatial resolution
 95 of 7 cm/px. Agisoft Photoscan uses Structure From Motion in a photogrammetric workflow
 96 with high levels of automation and good levels of data quality (Fonstad et al., 2013), see
 97 De Haas et al. (2014) for details on its application to the alluvial fan environment.

98 A surface particle-size map was made of multiple colluvial fans with the HRSC-AX
 99 images and ground truthing via photosieving, based on the methods of Carbonneau et al.
 100 (2004) and Carbonneau (2005), in which image texture (i.e., entropy) is correlated to the
 101 median size of the particles. This approach relies on variations of brightness values induced
 102 by surface particles. Larger particles cast larger, but localized, shadows thus leading to
 103 more variation and light/dark contrasts. This method requires an empirical calibration for
 104 each image data set. For a detailed description on the procedures for photosieving and
 105 application of this method to the alluvial fan environment the reader is referred to De Haas
 106 et al. (2014). Calibration results of HRSC-AX image entropy and median particle size are
 107 given in Figure 2.

108 Morphometric analyses of fans and catchments were performed in ArcMap 10. Fan and
109 catchment area were visually delineated from the aerial images and DEM. Catchment relief
110 was defined as the elevation difference between the highest point of the catchment and the
111 fan apex. Catchment length and slope were measured over a straight line connecting the
112 highest point in the catchment with the fan apex. Fan relief was defined as the elevation
113 difference between the fan apex and the lowest point at the fan toe. Fan length and slope
114 were measured over a straight line connecting these two points.

115 We conducted field site visits for geomorphological observations on fans in Adventdalen,
116 Bjørndalen, Longyeardalen, Hanaskogdalen and Mälardalen in August 2013 (Fig. 1). Pro-
117 cesses responsible for the fan morphology were identified by conventional field reconnaissance
118 (cf. Blair and McPherson, 1994; Blikra and Nemeč, 1998). The summer season of 2013 was
119 relatively wet, with a total amount of precipitation of 123 mm at Svalbard airport, compared
120 to 25 mm in 2011 and 50 mm in 2012. Hence, there was a relatively large amount of vege-
121 tation at the surface, and debris flows occurred on a few fans in our study area during the
122 fieldwork period, providing detailed insight into their formative processes and composition.

123 3. Svalbard climate, geology and geomorphic processes

124 3.1. Geological and climatic setting

125 The present climate of Svalbard is arctic with mean annual temperatures ranging be-
126 tween -6°C at sea level and -15°C in the high mountains. In the Adventdalen area the
127 coldest (February) and warmest (July) months have mean temperatures of -15.2°C and
128 6.2°C , respectively, and the mean annual air temperature is -5.8°C (Hanssen-Bauer and
129 Førland, 1998). Yearly average precipitation is low and reaches ~ 180 mm in central Spits-
130 bergen, whereas along the coast of Svalbard precipitation ranges between 400-600 mm. Snow
131 is the dominant precipitation type: around 75% of the precipitation events are snow at
132 Longyearbyen airport (Førland and Hanssen-Bauer, 2003). Interannual differences in mean
133 precipitation and temperatures can be high. Heavy snowfalls generally occur in Decem-
134 ber and January, and snow avalanches are frequent, especially on downwind slopes (Vogel
135 et al., 2012). Mean annual temperatures have increased by $\sim 1^{\circ}\text{C}$ per decade during the
136 last decades on Svalbard, while winter warming is even more dramatic, with an increase of
137 $2\text{-}3^{\circ}\text{C}$ per decade. Mean annual precipitation has increased with 2-4% per decade (Førland
138 et al., 2012). On average, the Adventdalen area has 5-14 days a month with winds stronger
139 than 14 m s^{-1} and up to 5 days with winds exceeding 25 m s^{-1} (Førland et al., 1997). The
140 strongest winds predominate in winter, and therefore snowpacks thicker than 1 m accumu-
141 late only in local wind shadows. Local wind shadows are mainly ravines, stream channels
142 and cornices, which are wedge-like snowdrifts that form on lee sides of ridges and slope in-
143 flexions (Latham and Montagne, 1970; Vogel et al., 2012; Eckerstorfer et al., 2012). About
144 60% of Svalbard is covered by glaciers and ice caps, whereas the remainder is characterized
145 by continuous permafrost (Brown et al., 1997). Surficial runoff of meltwater is limited to
146 two or three summer months, when it is accompanied by scarce rainfall (Lønne and Nemeč,
147 2004). Permafrost thickness is 10-40 m in coastal regions and ~ 100 m in major valleys, but
148 can increase to more than 450 m in the highlands (Liestøl, 1976; Sollid et al., 2000; Isaksen

149 et al., 2001). The active layer of the permafrost, the layer that annually thaws in summer
150 and is available for erosion, has a thickness of 0.4-1 m depending on topography (Åkerman,
151 1984; Christiansen et al., 2010; Harris et al., 2011). Permafrost surface temperatures have
152 increased by 0.5-2°C in the last century (Isaksen et al., 2000; Etzelmüller et al., 2011), and
153 the present decadal warming rate at the permafrost surface is in the order of 0.07°C yr⁻¹,
154 with indications of accelerated warming in the last decades (Isaksen et al., 2007). As a re-
155 sult, active-layer thickness has increased over the last decades (Åkerman, 2005; Etzelmüller
156 et al., 2011).

157 The Adventdalen region is dominated by an extensive plateau mountain massif, rising to
158 an average elevation of 450-550 m above sea level (a.s.l.). The highest peaks in the area reach
159 up to 1000 m a.s.l and have an alpine topography. The plateau mountains are separated by
160 glacio-fluvially eroded U-shaped valleys that deglaciated around 10,000 yr BP (Mangerud
161 et al., 1992; Svendsen and Mangerud, 1997), causing widespread paraglacial activity (André,
162 2003; Lønne and Nemeč, 2004; Mercier et al., 2009; Rachlewicz, 2010). Geologically, the
163 bedrock of the massifs bordering Adventdalen consists of Jurassic and Cretaceous sediments
164 that belong to the Helvetiafjellet and Carolinefjellet Formations (Dallmann et al., 2001,
165 2002). These formations are characterized by subhorizontal layers (centimeters to tens of
166 centimeters) of sandstones, siltstones, shales and some thin coal seams (Parker, 1967; Major,
167 1972). Bedrock weathering is driven mainly by frost (Lønne and Nemeč, 2004), producing
168 large amounts of weathered material, including abundant clays (Jahn, 1976; Sørbel et al.,
169 2011). The short distance from the high mountains to the ocean causes strong downstream
170 grain-size fining (Frings, 2008) from the fans into the large rivers and fan deltas in the fjords.
171 In the Adventdalen region loess (Bryant, 1982) and arctic meadow (Van Vliet-Lanoë, 1998)
172 soils are present, characterized by a high organic content. The low-sloping parts of the
173 region are covered by a moist open tundra vegetation (Rozema et al., 2006). Long-inactive
174 parts of alluvial fans are often vegetated. The steeper and geomorphologically more active
175 colluvial fans are unvegetated.

176 *3.2. Review of geomorphic processes on the periglacial slopes of Svalbard*

177 Slopes on Svalbard are mainly modified by a combination of rockfalls, snow avalanches,
178 debris flows, fluvial flows (i.e. stream flows and hyperconcentrated flows) and various slow
179 mass-wasting processes, of which solifluction is the most important (e.g., Rapp, 1960; Jahn,
180 1967; Larsson, 1982; Åkerman, 1984; André, 1990; Lønne and Nemeč, 2004; Siewert et al.,
181 2012; Eckerstorfer et al., 2013). Principal sources of flowing water are the melting of snow,
182 glaciers and the thawing of the active layer, combined with rain showers (e.g., Lønne and
183 Nemeč, 2004). These slope processes determine the water and sediment fluxes onto the fans
184 and are therefore briefly reviewed in this section. We especially focus on snow avalanches, as
185 these are common in periglacial and Alpine environments and therefore generally overlooked
186 in current alluvial-fan research.

187 *3.2.1. Snow avalanches*

188 Snow avalanches are very frequent on Svalbard and numerous snow avalanches are trig-
189 gered on a yearly basis in the Adventdalen region (e.g., Eckerstorfer and Christiansen,

190 2011a,b). The main types of snow avalanches are cornice-fall avalanches, slab avalanches,
191 loose snow avalanches and slush avalanches (Eckerstorfer and Christiansen, 2011b).

192 Most snow avalanches in the Adventdalen region are cornice-fall avalanches from cornices
193 that accumulated along plateau edges (45%) (Eckerstorfer and Christiansen, 2011b). Cornice
194 accumulation is caused by strong and continuous wind activity on the widespread plateau
195 mountains, which causes transport of snow across the plateaus. Cornices are today most
196 frequent on W-NW oriented slopes because of the prevailing regional SE wind direction in
197 the snow season (Eckerstorfer and Christiansen, 2011b; Vogel et al., 2012). Consequently,
198 snow-avalanche-induced sediment accretion rates on NW facing slopes are more than twice
199 as high as on SE facing slopes (Vogel et al., 2012; Eckerstorfer et al., 2013). Cornice-fall
200 avalanches generally occur on a yearly basis below many plateau edges (Eckerstorfer and
201 Christiansen, 2011b; Eckerstorfer et al., 2013). They mainly take place at the end of the
202 snow season around June, when tension cracks develop and grow between the cornice mass
203 and the plateau (Vogel et al., 2012). Cornices are thus able to significantly erode the plateau
204 edge and rockwall during their formation (a process termed ‘cornice plucking’; Vogel et al.,
205 2012; Eckerstorfer et al., 2013).

206 Slab avalanches are the second most dominant, and generally largest, snow avalanche
207 type (32%), releasing equally on all slope aspects (Eckerstorfer and Christiansen, 2011b).
208 These avalanches result from failure in a weak layer or interface, generally consisting of a
209 thin layer of hoar formed by condensation of water vapour (e.g., Jamieson and Schweizer,
210 2000), underlying a cohesive slab layer. They are mainly triggered by additional snow
211 loading as well as distinctive cooling or warming of the upper snow layers (Eckerstorfer and
212 Christiansen, 2011b).

213 Loose snow avalanches (22% of recorded snow avalanches) often result from failure of
214 snow that has been deposited at a steeper angle than the natural angle of repose of snow,
215 typically $\sim 30^\circ$ (Blikra and Nemec, 1998; Eckerstorfer and Christiansen, 2011b). They usu-
216 ally start at a point or small area and expand as they move, implying that more snow is
217 entrained in the process and that the presence of loose snow is a necessary condition. The
218 majority of loose snow avalanches occur at the end of the snow season, releasing mainly on
219 south facing slopes due to the higher direct solar radiation (Eckerstorfer and Christiansen,
220 2011b).

221 Slush avalanches only comprise a minor percentage of the total amount of snow avalanches
222 (1%), but do occur on a yearly basis in the Adventdalen region (Eckerstorfer and Chris-
223 tiansen, 2011b, 2012). Slush avalanches typically occur in arctic regions. They are triggered
224 by an increase in the content of free water in the snowpack which decreases snowpack
225 strength (Nyberg, 1989). The free water increase can be caused by intensive spring melting
226 of snow and/or rain on snow events (e.g., Jahn, 1967; André, 1995; Hestnes, 1998; Decaulne
227 and Sæmundsson, 2006), and is exacerbated by an impermeable permafrost table that acts
228 as an aquiclude. In contrast to dry snow avalanches, wet slush avalanches can be generated
229 on slopes as low as 10° (Blikra and Nemec, 1998). The vast majority of slush avalanches
230 move through narrow gorges, where snow accumulates and persists longer into the melting
231 season, and flow out onto alluvial fans (Eckerstorfer and Christiansen, 2012).

232 Snow avalanches can have a considerable geomorphic effect if they are able to erode sed-

233 iment (e.g., Luckman, 1977; Åkerman, 1984; Nyberg, 1989; André, 1990; Blikra and Nemec,
234 1998; Decaulne and Sæmundsson, 2006; Eckerstorfer et al., 2013; Laute and Beylich, 2014).
235 However, only a limited subset of all snow avalanches accomplish significant sediment trans-
236 port: most snow avalanches only redistribute the surface snow cover without coming into
237 contact with the underlying ground surface. Avalanche erosion only occurs when avalanches
238 run over bare ground or involve the full depth of the snow cover (e.g., Luckman, 1977).
239 Vegetation cover may also protect the underlying surface from erosion. Hence, the erosion
240 potential of avalanches is highest on loose, unconsolidated debris mantles covered by no or
241 a limited amount of snow (Luckman, 1977). Therefore, cornice fall and slush avalanches
242 have the largest geomorphic effect (André, 1990; Eckerstorfer et al., 2013), as they regularly
243 occur at the end of the snow season from retained snow accumulations at the top of slopes
244 and in couloirs, ravines and gullies, while their surroundings are free of snow or covered by
245 a thin layer of snow only.

246 Important morphological indicators for snow avalanche erosion and sedimentation are
247 perched or balanced cobbles and boulders, which came to rest on top of each other after
248 melting of the snow avalanches (Rapp, 1960; Luckman, 1977, 1992; Decaulne and Sæmunds-
249 son, 2006), arcuate accumulations of debris, bulldozed ahead by avalanches marking the base
250 of the avalanche track (Rapp, 1960; Luckman, 1977; Jomelli and Francou, 2000), debris-tails,
251 tails of debris that are present in the lee of large immobile obstacles, generally cobbles or
252 boulders, where erosion is prevented (Blikra and Nemec, 1998) and debris-horns, accumu-
253 lated sediment on the upslope side of immobile obstacles due to local plastic freezing of
254 avalanches rich in sediment (Blikra and Nemec, 1998). Moreover, steep mountain walls of
255 snow avalanche-dominated upper catchments are often dissected by narrow parallel or funnel
256 shaped avalanche chutes, which are rounded valleys with an open, flat-bottomed, U-shaped
257 cross profile that formed by pervasive avalanche erosion (e.g., Rapp, 1960; Luckman, 1977).

258 3.2.2. *Rockfall*

259 Rockfall, the downward falling, rolling or skipping of rock fragments under the force of
260 gravity, is a common process on Svalbard. Bedrock on Svalbard is mainly exposed to frost
261 weathering (e.g., Matsuoka, 1991), thereby releasing rock from cliff faces and delivering con-
262 siderable amounts of sediment to talus slopes or, if funnelled, colluvial fans (e.g., Rapp, 1960;
263 Jahn, 1967, 1976; Larsson, 1982; Åkerman, 1984; André, 1986, 1990, 1997; Siewert et al.,
264 2012). Rockwall weathering and erosion rates mainly depend on rockwall lithology, aspect,
265 elevation and erosional processes. Due to the weak to moderate rock mass strength of the
266 sedimentary sandstones, siltstones and shales in the Adventdalen region, rockwall weather-
267 ing rates and rockfalls are among the highest on Svalbard and other arctic regions (Siewert
268 et al., 2012). Sediments are eroded by a combination of frost-weathering and subsequent
269 rockfall (Siewert et al., 2012; Eckerstorfer et al., 2013), cornice plucking (Vogel et al., 2012)
270 and rockwall erosion by avalanches (Humlum et al., 2007; Siewert et al., 2012; Eckerstor-
271 fer et al., 2013). Rockwall retreat rates on Svalbard significantly decreased after an initial
272 paraglacial increase since deglaciation (André, 1997, 2003), and colluvial fan accumulation
273 rates decreased accordingly. However, on steep northwest-facing slopes where large snow
274 cornices develop rockwall retreat rates remain similar to early paraglacial retreat rates, due

275 to the present intensive erosion by cornice-fall avalanches (Vogel et al., 2012; Eckerstorfer
276 et al., 2013).

277 *3.2.3. Debris flows*

278 Debris flows are abundant on steep slopes on Svalbard. Bedrock weathering in the
279 Adventdalen region, mainly comprising sedimentary sandstones, siltstones and shales, yields
280 a wide range of sediments including many fines (i.e., silt and clay), which is ideal for the
281 formation of debris flows in combination with the steep hillslopes and permafrost ground
282 (e.g., Blair, 1999; Harvey, 2010). The debris flows in this region are mainly triggered by
283 heavy rainstorms in summer (Bibus, 1975; Thiedig and Kresling, 1973; Larsson, 1982; Rapp,
284 1985), but rapid snowmelt has also triggered large debris flows in a few known cases (Rapp,
285 1986). Permafrost slopes, especially in arctic fine-grained soils (Harris and Lewkowicz, 2000;
286 Lewkowicz and Harris, 2005), are prone to slips and slides. This is caused by the permafrost
287 table which acts as an aquiclude and a potential failure plane during periods of elevated pore
288 pressure (i.e. active-layer detachment), after summer rainfall events or extreme thaw periods
289 (e.g., Larsson, 1982; Sattler et al., 2011). The co-existence of frozen and unfrozen moisture
290 in soil-voids close to the seasonally shifting thawing plane increases the probability of active-
291 layer failure (Nater et al., 2008). In these permafrost conditions, rainfall intensities as low
292 as 2.5 mm/h can cause debris flows (Larsson, 1982), which is a much lower threshold than in
293 other climatic regions (Caine, 1980). André (1990) found that debris flows on Svalbard are
294 relatively small-sized because of the limited active-layer depth (0.4-1 m; Åkerman, 1984;
295 Christiansen et al., 2010). Such a limited active-layer depth restricts debris-flow volume
296 by limiting the volume of debris available for remobilization. The largest debris flows are
297 most likely to occur in mid to late summer, when the active-layer depth is at its maximum
298 and shear forces on the slopes are close to the threshold for failure, especially after periods
299 of longlasting rain. For example, 30.8 mm precipitation during a 12 h period between
300 10 and 11 July 1972 triggered many debris flows in the Adventdalen region (Thiedig and
301 Kresling, 1973; Jahn, 1967; Larsson, 1982). However, these catastrophic events occur rarely
302 on Svalbard due to the infrequent occurrence of heavy rainfalls (André, 1990; André, 1995;
303 Reiss et al., 2011). Debris-flow return periods were tentatively estimated from lichenometry
304 at 80 to 500 years in northwestern and central Svalbard (André, 1990; André, 1995), but are
305 probably higher on most of the studied fans in the Adventdalen region, given the pristine
306 morphology and lack of lichen and vegetation on many debris-flow deposits.

307 *3.2.4. Fluvial flows: stream and hyperconcentrated flows*

308 Fluvial flows appear to only have a minor geomorphic effect on steep slopes on Svalbard.
309 However, small incised channels on talus slopes and fans continuously convey small amounts
310 of discharge from snowmelt in spring and summer. Snow patches survive until late summer in
311 sheltered depressions like gully-head alcoves. Even in late summer, these snow patches feed
312 small streams within gullies and fans (Reiss et al., 2011). Additionally, fluvial flow from
313 higher parts of the slopes can load remnant snow patches with excess water, potentially
314 inducing slush avalanches. During snowmelt drainage is often concentrated on the slope
315 surface due to the shallow active-layer depth, testified by many rills on the slopes (Larsson,

316 1982). Fluvial flows mainly have significant geomorphic importance on fans with relatively
317 large and low sloping catchments as well as valley bottoms (e.g., Bogen and Bønsnes, 2003;
318 Lønne and Nemeč, 2004; Szpikowski et al., 2014), where relatively large amounts of water
319 are able to concentrate. Paraglacial activity (Lønne and Nemeč, 2004; Mercier et al., 2009;
320 Rachlewicz, 2010) following the last major deglaciation has caused extensive fanhead incision
321 on many fluvial fans on Svalbard (Lønne and Nemeč, 2004). These fans are fed by large
322 catchments, where cirque glaciers were generally present during glacial periods. After retreat
323 of these glaciers, large amounts of sediment were ready for transport and fan construction,
324 but when sediment supply from the catchments ceased, fan aggradation rates decreased
325 accordingly, leading to the large fan incisions (Lønne and Nemeč, 2004).

326 3.2.5. *Slow mass-wasting*

327 Solifluction is the dominant form of slow mass wasting on Svalbard (e.g., Åkerman, 1984;
328 Harris et al., 2011). It depends on seasonal frost heave, thaw consolidation of the active
329 layer and snowmelt and rainfall in summer, resulting in saturation and movement of the
330 upper surface soil layer (Matsuoka, 2001; Harris et al., 2011). Solifluction landforms are
331 widespread on Svalbard, and include extensive solifluction sheets, sorted and non-sorted
332 solifluction lobes, stripes and steps or terraces, hummocks and talus creep (e.g., Jahn, 1967;
333 Åkerman, 1984; Matsuoka and Hirakawa, 2000; Sørbel and Tolgensbakk, 2002; Åkerman,
334 2005; Harris et al., 2011; Johnsson et al., 2012). Movement of solifluction lobes and sheets
335 ranges between 2-5 cm yr⁻¹ across Svalbard (Jahn, 1976; Sørbel and Tolgensbakk, 2002;
336 Matsuoka and Hirakawa, 2000; Åkerman, 2005; Harris et al., 2011), whereas movement
337 outside solifluction lobes is lower and generally does not exceed 0.7 cm yr⁻¹ (Sørbel and
338 Tolgensbakk, 2002). Solifluction rates are highest on steep talus slopes; at Kapp Linné
339 talus creep caused an average surface displacement of 8.9 cm yr⁻¹ between 1972 and 2002
340 (Åkerman, 2005).

341 3.2.6. *Relative effectiveness of slope processes*

342 The slope processes reviewed above rarely act in isolation and the dominant geomor-
343 phic processes differ from one slope or catchment to the other, depending among others on
344 lithology, meteorology, slope and aspect. On many slopes solifluction is the dominating mass-
345 wasting process on a year-to-year basis (Matsuoka, 2001; Åkerman, 2005), while episodic and
346 rapid processes (e.g., debris flows and snow avalanches) are much more important in terms
347 of total long-term mass movement (Åkerman, 2005). Although the transported amount of
348 sediment per dry snow avalanche is generally much lower than per debris flow, fluvial flow
349 or slush avalanche, the much higher frequency of cornice avalanches on steep slopes below
350 the plateau mountains results in a larger geomorphic effect of cornice avalanches on most
351 of these slopes (Eckerstorfer et al., 2013). This suggests that rockfall and snow avalanches
352 are important sediment transport mechanisms on Svalbard fans below steep catchments and
353 rockwalls, whereas debris flows, fluvial flows and slush avalanches are more abundant on
354 fans below lower sloping catchments.

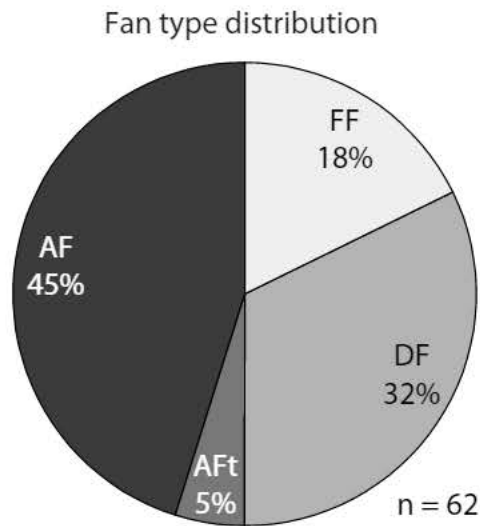


Figure 3: Breakdown of fans by dominant formative mechanism (Table 1). Fan type abbreviations: AF = cone-shaped snow avalanche-dominated colluvial fan, AFt = tongue-shaped snow avalanche-dominated colluvial fan, DF = debris-flow-dominated fan, FF = fluvial-flow-dominated fan.

355 4. Observations on morphology and morphometry of fans on Svalbard

356 Three main types of fans were distinguished in the study region: (1) colluvial fans mainly
 357 formed by snow avalanches and additional rock falls, but with a snow avalanche-dominated
 358 morphology (AF and AFt), (2) alluvial fans dominantly formed by debris flows (DF) and
 359 (3) alluvial fans dominantly formed by fluvial flows (FF) (Fig. 3; 4; Table 1; Fig. S1-S6).
 360 Below the morphology and morphometry of these fan types are described to identify the
 361 various contributions of the slope processes described above to fan formation and to identify
 362 the effect of periglacial (snow- and permafrost-related) processes on these fans.

363 4.1. Morphometry

364 There is a strong distinction between fan slope versus catchment area, and fan area versus
 365 catchment area relations between the rockfall and snow avalanche-, debris-flow- and fluvial-
 366 flow-dominated fans on Svalbard (Fig. 5). The colluvial fans have a smaller fan area and
 367 catchment area and are steeper than the debris-flow- and fluvial-flow-dominated fans. The
 368 slope and area of the debris-flow- and fluvial-flow-dominated fans are in the same range.
 369 The main morphometric difference between these two fan types is their catchment: the
 370 fluvial-flow-dominated fans have a larger catchment area and a lower slope (Table 1). This
 371 implies that the dominant formative process of fans on Spitsbergen is largely determined by
 372 catchment morphometry. More rain or meltwater is able to accumulate in larger catchments
 373 and less sediment can be entrained because of the lower slope, resulting in a smaller sediment
 374 to water ratio and fluvial flows. The morphometry of the fans on Svalbard is within the
 375 range observed in various arid to semi-arid regions in Spain and the United States (Harvey,

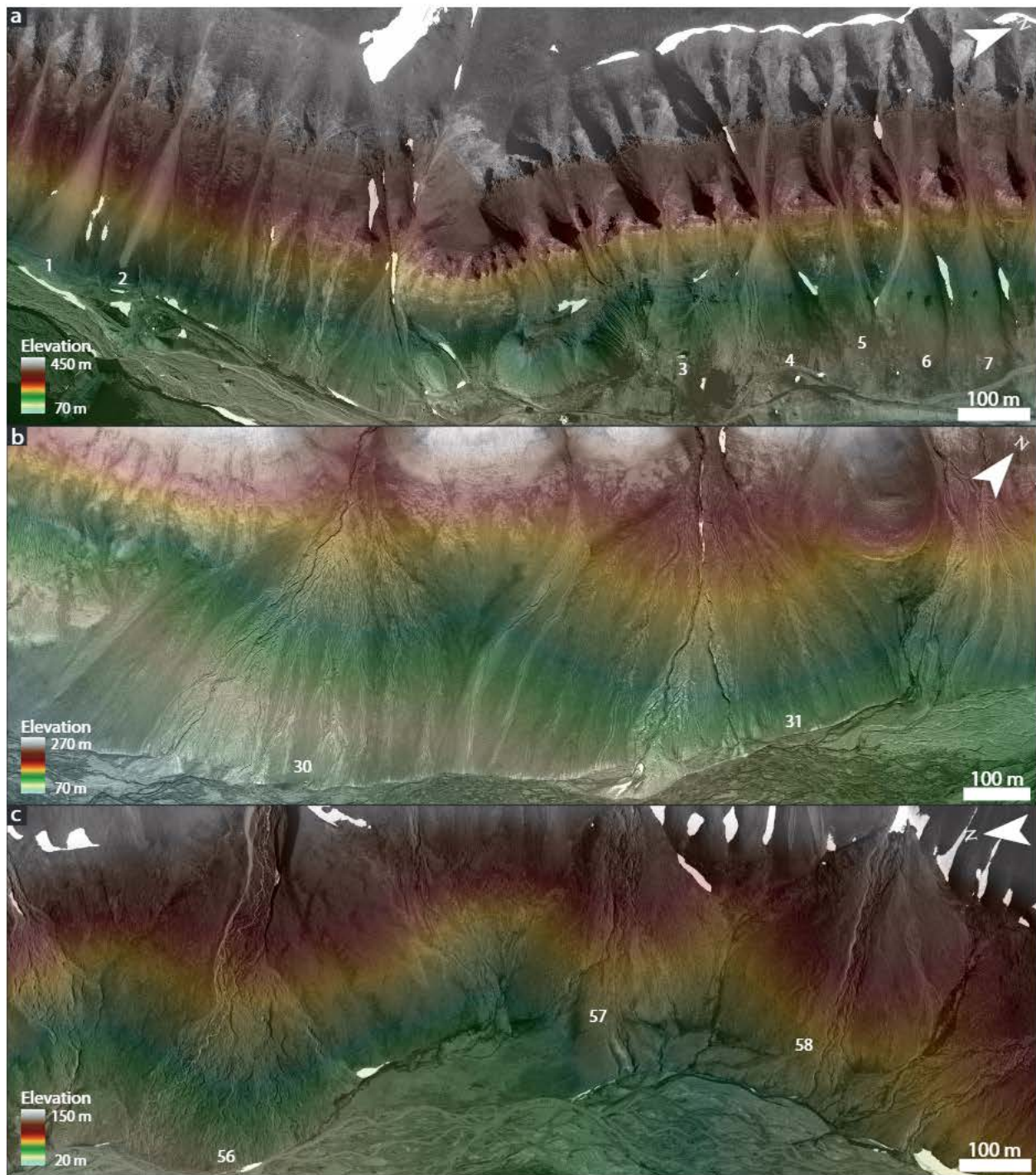


Figure 4: Fan types in the Adventdalen region. (a) Colluvial fans in Longyeardalen (fan 1-7). (b) Debris-flow-dominated fans in Mälardalen (fan 30-31). (c) Fluvial flow-dominated fans in Bjørndalen (fan 56-58). See Table 1 for corresponding fan numbers and details.

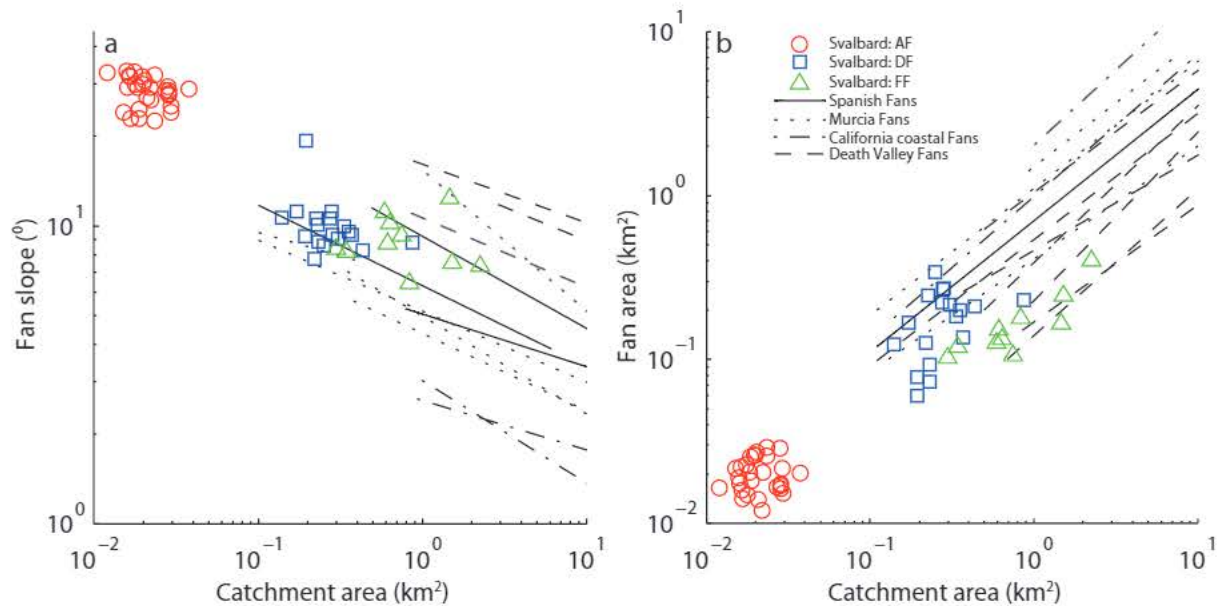


Figure 5: Comparison between Svalbard fan morphometry and fans in other environments. (a) Fan slope versus catchment area. (b) Fan area versus catchment area. Data from fans in other environments from Harvey (2011). See Table 1 for raw data.

2011), which suggests that there are no substantial climate-specific differences in large-scale fan morphometry between periglacial and other environments.

4.2. Snow avalanche-dominated fans

Svalbard hosts many colluvial fans, which have formed by a combination of snow avalanches and rockfall (Fig. 6a,b,d). Although the relative influence of both processes differs between sites, snow avalanches dominate the morphology of the studied colluvial fans. These fans are steep ($\sim 29^\circ$) and small, and are typically fed by short and steep ($\sim 39^\circ$) catchments with a sharp plateau edge, where cornice formation and corresponding cornice-fall avalanches are frequent (Table 2). Fan long-profiles are concave, whereas cross-profiles are plano-convex, but with a flattened top because of snow avalanche erosion, especially in the proximal domain of the fans (Fig. 6a-c). The steep mountain walls of the upper catchment and the fan deposits are often dissected by narrow parallel or funnel-shaped snow avalanche chutes. Snow avalanches especially erode large particles that stick out of the surface. Therefore, the proximal fan surface often comprises relatively fine sediments, ranging from clay to small cobbles (Fig. 7e), whereas coarse material, up to 0.5 m in diameter, is deposited on the distal domain of the fans (Fig. 7g; 8). The voids between the pebbles and small cobbles on the proximal domain are filled with fine sediments, as snow avalanche erosion continuously exposes the deeper talus, whereas the coarse material on the distal domain generally has an openwork texture. On the non-flattened sides of the proximal domain of the fan coarse, openwork debris is also abundant, as these parts of the fan are sheltered from snow avalanche erosion. Arcuate alignments of coarse sediment mark the limit of past avalanche activity on

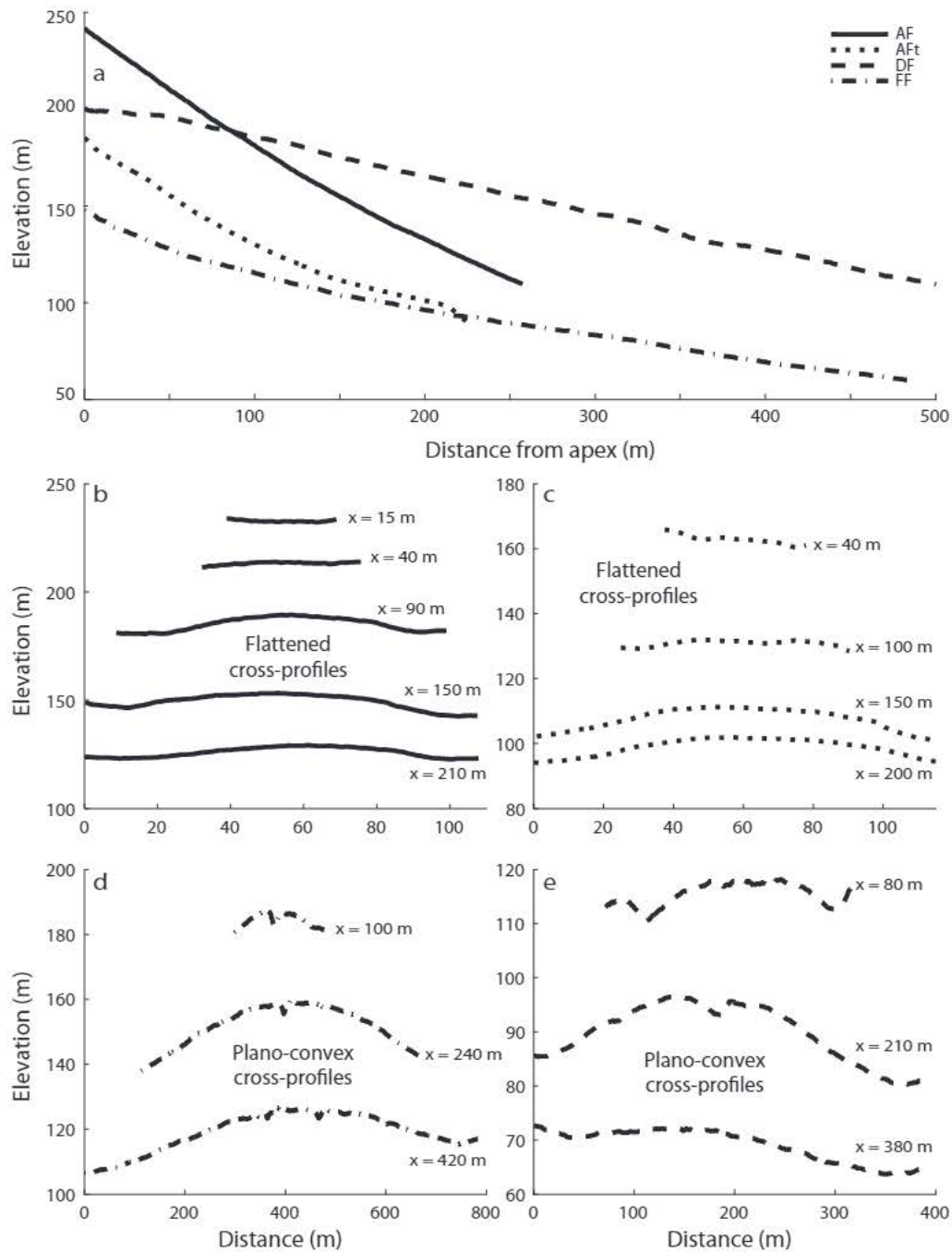


Figure 6: Topographic profiles (above MSL) of selected examples of the discriminated fan types. (a) Long-profiles of cone-shaped snow avalanche-dominated colluvial fan (AF; fan 7), tongue-shaped snow avalanche-dominated colluvial fan (AFt; fan 53), debris-flow-dominated fan (DF; fan 31) and fluvial-flow-dominated fan (FF; fan 58). (b) Cross-profiles of cone-shaped colluvial fan. (c) Cross-profiles of tongue-shaped colluvial fan. (d) Cross-profiles of debris-flow-dominated fan. (e) Cross-profiles of fluvial-flow-dominated fan. Distance from apex denoted by 'x'. Based on HRSC-AX data.

397 some colluvial fans (Fig. 7a). There is a sharp color transition between the freshly exposed
398 proximal domain of the fans and the older, coarse debris along the edges and distal domain
399 of the fans, where sediment has become grayer due to lichen growth and rock varnish. The
400 extensive sediment transport by snow avalanches on the fans is testified by the widespread
401 occurrence of perched cobbles and boulders on all colluvial fans (Fig. 7g). Moreover, debris-
402 tails (Fig. 7d) and debris-horns (Fig. 7f) were found on the proximal domain of some of the
403 colluvial fans. On distal surfaces where vegetation was removed by snow avalanches, roots
404 were oriented in the flow-direction of the erosive snow avalanches.

405 On all studied colluvial fans we found many of the above indicators (i.e., flattened cross-
406 profiles, heavily eroded apex region, perched boulders) of extensive snow avalanche activity,
407 suggesting that snow avalanches dominantly affect the morphology of all colluvial fans in the
408 Adventdalen region. Siewert et al. (2012) show that the prevailing SE wind direction causes
409 colluvial fans on NW facing slopes to be dominantly aggraded by snow avalanches, while
410 the colluvial fans on the SE facing slopes dominantly aggraded by rockfall. This suggest
411 that snow avalanches dominate the surface morphology and texture off all colluvial fans in
412 the region regardless of their dominant aggradational mechanism.

413 Three out of 31 investigated colluvial fans have a typical tongue-shape (Fig. 7a,b), often
414 referred to as roadbank tongue (Rapp, 1960; Luckman, 1977) or boulder tongue (Jomelli and
415 Francou, 2000). These tongue-shaped deposits have a marked basal concavity of the lower,
416 depositional, part of the fan, and a flat-topped vertical profile, not only in their proximal
417 but also in their distal domain (Fig. 6c). More importantly, the distal domain of the tongue
418 generally has a relatively low-sloping longitudinal profile and the lower edge of the tongue
419 is often marked by a typical step of a few meters in height. As such, these fans have a
420 relatively large difference in apex zone and distal zone angle. Consequently, their average
421 slope can be as low as 15° (Table 2). Whether a cone- or tongue-shaped colluvial fan is
422 formed appears to be controlled by sediment supply. Where sediment supply is high, and a
423 large amount of sediment has accumulated on a fan, snow avalanches continuously rework
424 and bulldoze previously deposited sediment towards the lower fan, eventually forming the
425 marked tongue-shaped deposit. Although deposition or erosion may occur on any part of
426 the tongue per snow avalanche, the overall effect is a net downslope transfer of sediment
427 forming the marked tongue-shaped deposit. On fans where less material has accumulated,
428 no tongue-shaped front develops.

429 On the majority of the snow avalanche-dominated fans, one or two debris-flow tracks
430 are present originating from the upper parts of the fans, where a mixture of angular de-
431 bris and fines is exposed. However, after formation the marked relief of the paired levees
432 and depositional lobes is rapidly bevelled and levelled by the erosional effect of subsequent
433 snow avalanches. Moreover, where levees still have a marked relief much snow avalanche-
434 transported debris accumulates in between the levees, where it is sheltered from erosion
435 by subsequent snow avalanches. Solifluction and creep are prevalent on the steep snow
436 avalanche-dominated fans in Svalbard (Fig. 9). They transport debris downslope and mod-
437 ify original fan morphology. Solifluction sheets are evident at the base of some of the steep
438 snow avalanche-dominated fans (Fig. 9a). Small solifluction lobes have developed at the
439 surface of some of these fans, but mainly on fans where the primary input of debris from

Table 2: Summary of morphometric characteristics per fan type. Total number of investigated fans is given behind fan type abbreviation. Area and slope values are median, minimum and maximum, respectively. See Table 1 for raw data.

Fan type	Fan slope, °	Fan area, m ²	Catchment slope, °	Catchment area, m ²	Long-profile	Cross-profile
AF (28)	29 (23-34)	19733 (11366-29270)	39 (36-43)	20282 (7489-37922)	concave	plano-convex, with a flattened top
AFt (3)	23 (15-29)	16098 (16098-16805)	32 (32-38)	17620 (14151-60410)	concave, with marked basal concavity	plano-convex, with a flattened top
DF (20)	9 (8-19)	175928 (21757-341782)	25 (15-32)	262764 (139670-869820)	straight to slightly concave	plano-convex
FF (11)	9 (7-12)	133935 (77040-403853)	11 (7 - 23)	693672 (297860-225486)	concave	plano-convex

440 snow avalanches and rockfall is limited (Fig. 9a). On fans where debris supply from snow
 441 avalanches and rockfall is larger solifluction occurs probably at similar rates, but is unable
 442 to develop lobes. Here, the formation of solifluction lobes is inhibited by the large input
 443 of debris by snow avalanches and rockfall together with snow avalanche erosion. This is
 444 illustrated on steep fans in Bjørndalen, where solifluction lobes are absent on the surfaces
 445 of snow avalanche fans where deposition and erosive events are frequent, but are present on
 446 the less active slopes between these fans (Fig. 9b).

447 4.3. Debris-flow-dominated fans

448 The average slope of the investigated debris-flow-dominated fans is 9° and they are
 449 typically between 400-700 m long and wide (Table 2). Longitudinal profiles are straight to
 450 slightly concave, and cross-profiles are typically plano-convex (Fig. 6a,d). In a few cases
 451 longitudinal profiles are convex in the proximal domain, potentially caused by rockfall or
 452 short dry snow avalanche input. Catchment length varies from 800 to 1700 m, and slopes
 453 average 25°. The majority of the debris-flow-dominated fans are eroded at their toe by
 454 valley-floor braided rivers, and many debris-flow channels reach the distal end of the fans
 455 or the valley-bottom braided rivers. Continuous snow and ice melt in the active layer
 456 within the catchments during spring and summer feeds small streams that flow through, and
 457 erode, the most recent debris-flow tracks on the fan surface. Consequently, these debris-flow
 458 tracks become significantly deepened (Fig. 10b,c), and subsequent debris flows are directed
 459 and transported within these channels. The small meltwater streams often bifurcate where
 460 debris-flow lobes plugged the channel (Fig. 10g). The investigated debris flows are rich in
 461 platy debris and clay, as seen in recent debris flows (1-3 days old) observed in Adventdalen,
 462 Mälardalen and Hanaskogdalen (Fig. 10d,f). The platy, coarse, debris is provided by the
 463 sandstone layers within the catchments, whereas the fines are provided by the shales and
 464 siltstones. Due to the platy shape of much of the coarse material, debris-flow lobes often show
 465 moderate to good imbrication. Furthermore, many centimeter to decimeter-sized blocks
 466 of ice are present within recent deposits, suggesting debris-flow formation by active-layer
 467 detachment. The main channel incision near the apex of the fans results in preferential
 468 debris-flow activity on a laterally restricted active part of the fan, and in the presence of
 469 extensive inactive parts. Levees are generally up to 3 m wide and up to 0.5 m high. However,



Figure 7: Snow avalanche-dominated fans. (a) Tongue-shaped snow avalanche fan (32) in Mälardalen. Note the snow avalanche flattened proximal domain, and the more grayish (more lichen) sediment along the sides and lower part of the fan. Arrows denote arcuate alignments of coarse sediment. Letters denote picture locations. (b) Tongue-shaped avalanche fan in Bjørndalen (fan 53). Note that the steepness of the step at the base of the fan is enhanced by basal erosion by the river. (c) Cone-shaped avalanche fans (5-9) in Longyeardalen. (d) Debris-tail on the proximal domain of fan 32. Hammer for scale. Black arrow denotes flow direction. (e) Fine-grained texture due to avalanche erosion on the proximal domain of fan 32. Black arrow denotes flow direction. (f) Debris horns on the proximal domain of fan 6 in Longyeardalen. White arrows point at the debris horns, black arrow denotes flow direction. (g) Accumulation of coarse sediment on the distal domain of fan 32. (h) Perched boulder on fan 32.

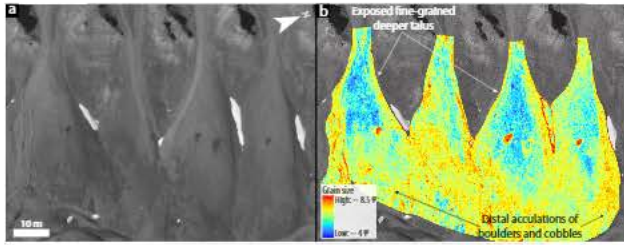


Figure 8: Surface texture of snow avalanche-dominated colluvial fans in Longyeardalen (fan 4-7). (a) HRSC-AX orthophoto. (B) Grain size maps on top of HRSC-AX orthophoto. Grain-size calibration curve in Figure 2.

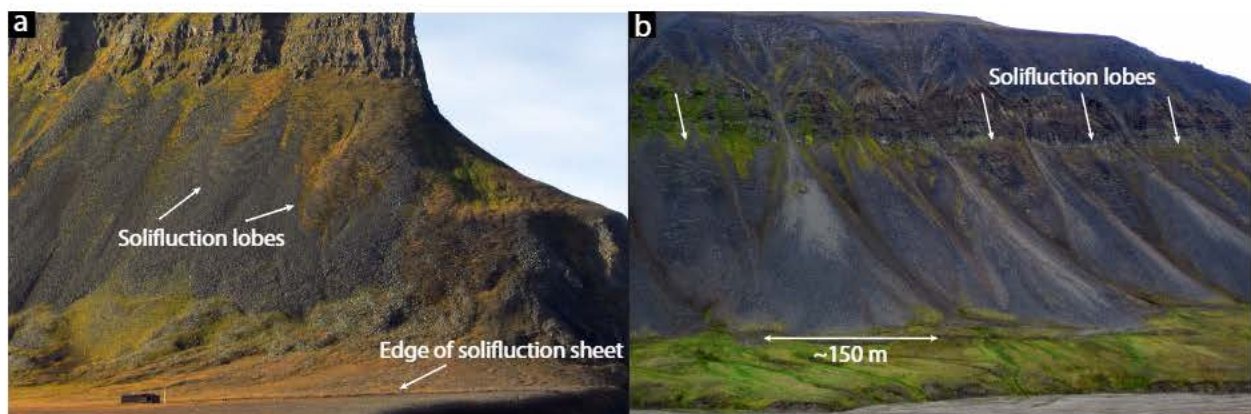


Figure 9: Solifluction lobes on fans. (a) Solifluction lobes on relatively inactive snow avalanche- and rockfall-dominated fans at the western side of Bjørndalen. A sharp-edged solifluction sheet is present at the foot of the fans. (b) Solifluction lobes on steep slopes between snow-avalanche dominated fans in Bjørndalen (fan 50-52).

470 older levees show much less relief, and ultimately become completely bevelled and levelled
471 (Fig. 10e; 11). Relative age estimations from lichenometry (Werner, 1990; Roof and Werner,
472 2011) indicate that levees become more bevelled with increasing age. Bevelling and levelling
473 can probably be attributed to the erosive effect of snow avalanches, solifluction and frost
474 weathering, although André (1990) and André (1995) mainly attribute it to snow avalanches.
475 No active-layer detachments were found that could be directly linked to debris-flow deposits
476 because we did not investigate the often steep catchments of the fans in the study area. To
477 illustrate the typical morphology of active-layer detachments we show examples found near
478 the mouth of Hanaskogdalen, and on steep slopes near Svea, 60 km south of Longyearbyen
479 in Figure 12.

480 The effect of snow avalanches on the fans is twofold, as they erode the fan surface, but can
481 also transport sediment to the fans, as testified by a recent slush-avalanche deposit on the
482 surface of a debris-flow-dominated fan in Adventdalen (Fig. 13), which forms a relatively
483 thin ($\sim 10\text{-}20$ cm), uniform blanket of sediment ranging in size from clay to cobbles and
484 boulders on a large part of the fan. In addition to erosion of debris-flow morphology by
485 snow avalanche erosion on the inactive parts of the fans, they are also heavily influenced
486 by other secondary processes (Fig. 15). Solifluction smooths the surface and causes slow
487 downfan transport of the fan material. Its effect is mainly testified to the formation of
488 solifluction lobes and sheets (vertical step of a few decimeters to a meter) at the distal end
489 of some of the fans (Fig. 15e). Furthermore, ice-wedges and associated polygonal ground
490 (up to ~ 10 m in diameter) are formed on inactive fan surfaces (Fig. 15a,b), and surface
491 sediments are broken down by frost weathering (Fig. 15f).

492 4.4. *Fluvial-flow-dominated fans*

493 The fluvial-flow-dominated fans have slopes ranging between 7° and 12° , their longitu-
494 dinal profiles are strongly concave (Fig. 6a,e), whilst cross-profiles are plano-convex. The
495 fans have a similar size as the debris-flow-dominated fans, whereas their catchments are
496 generally larger (Table. 2). Average catchment slope is 11° . Most fluvial-flow-dominated
497 fans are eroded at their toe by valley-floor braided rivers, and all such fans have a large apex
498 incision (up to 7 m deep) (Fig. 14a,b). In spring and summer there is continuous discharge
499 from the catchments from snow and permafrost melt. The incised morphology of these fans
500 causes a sharp separation between active and inactive sectors on the fan. The active part
501 shows a typical braided planform (Fig. 14b,c). The low flow is often critical or supercritical
502 with many static hydraulic jumps over immobile sediment and infrequent flow bifurcations
503 on an otherwise dry fan surface. Grain size on the fans varies from clay, silt and sand to
504 cobbles of 20-30 cm in diameter at maximum, and the largest fractions are clearly imbricated
505 (Fig. 14d). Sorting is quite patchy at scales smaller than typical bar wavelengths. Bar heads
506 are often heavily armoured by coarse, imbricated sediment, whilst backwaters preserved finer
507 sediments. The inactive part of the fans is smoother, most likely because of avalanche ero-
508 sion, is often vegetated and hummocks (up to ~ 5 m in diameter) and ice-wedge polygons
509 are present on long-inactive areas (Fig. 15c,d; Fig. 14e). On some fluvial-flow-dominated
510 fans there is also a significant geomorphic contribution of slush avalanches, as evidenced by
511 recent snow avalanche deposits on some of these fans (Fig. 13c).



Figure 10: Debris-flow-dominated fans. (a) Debris-flow-dominated fan (31) in Mälardalen. (b) Debris-flow channel, incised by meltwater stream. (c) Formerly incised debris-flow channel. Step-pool morphology implies reworking by runoff. Hammer for scale. (d) Very recent (1-3 days) debris flow on fan 30. (e) Heavily bevelled debris-flow on fan 31. (f) Very recent (1-3 days) debris flow on fan 34. (g) Bifurcated meltwater stream in debris-flow channel on fan 31. Meltwater streams often bifurcate and leave debris-flow channels where flow is ponding behind a debris-flow lobe.

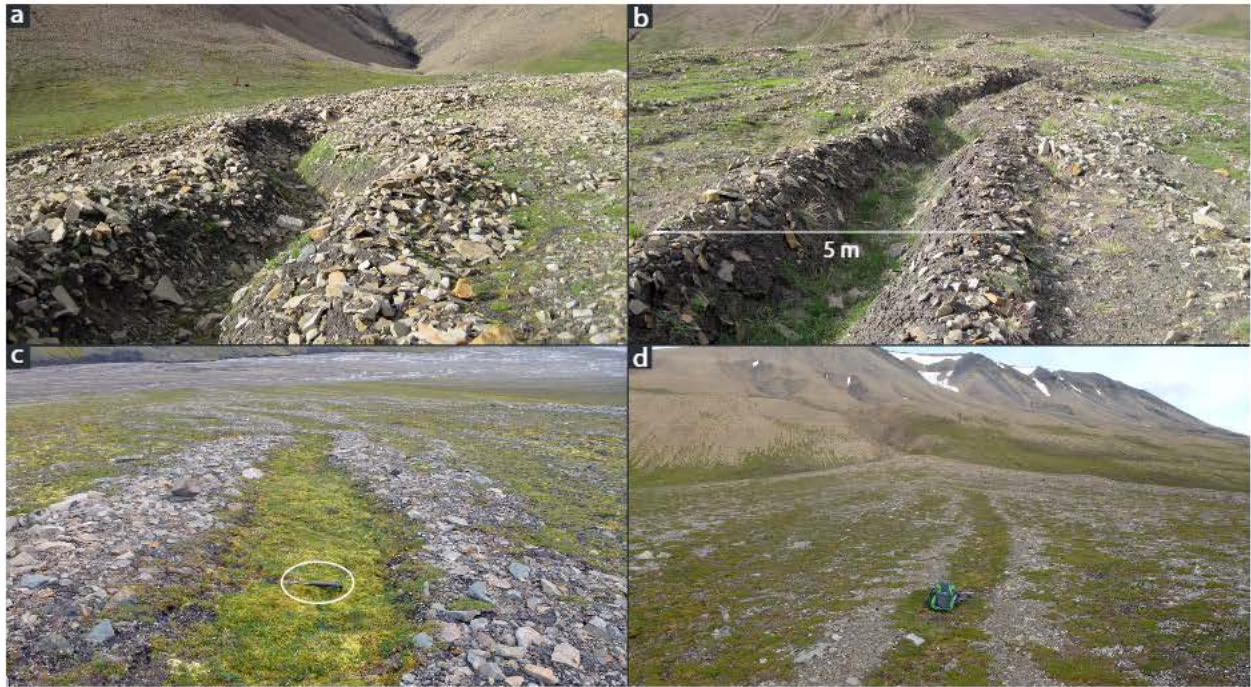


Figure 11: Debris-flow channels of different age and degree of beveling. (a,b) Relatively young debris-flow channels, with pronounced levees and deepened channels by meltwater erosion. Picture a is taken on fan 30, picture b on fan 31 in Mälardalen. (c,d) Relatively old, heavily bevelled debris-flow channels, on which relief is decreased to <math><10\text{ cm}</math>. Picture c from fan 30 in Mälardalen, picture d from fan 40 in Adventdalen (Table. 1).

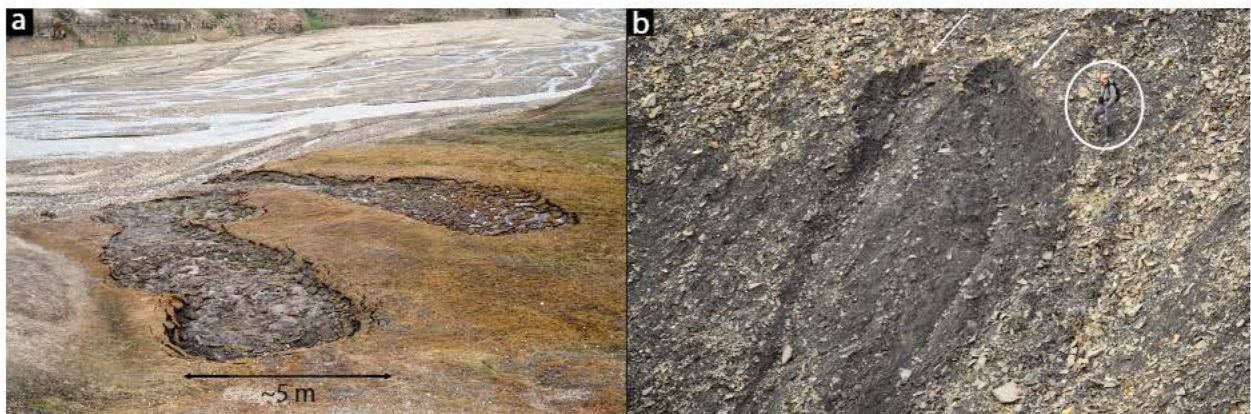


Figure 12: Examples of active layer detachment. (a) Active-layer detachment or thaw slump near the mouth of Hanaskogdalen. (b) Active-layer detachment on a steep slope near the mining town of Svea.



Figure 13: Recent slush-avalanche deposits. (a) Recent slush-avalanche deposit (<0.5 year) on a debris-flow-dominated fan in Adventdalen (fan 34; Table. 1). (b) Detail of slush-avalanche deposit, showing the wide range of sediment that was transported within the avalanche, and a prominent perched boulder. (c) Slush avalanche on a fan in Adventdalen, indicating the limited thickness of such deposits ($\sim 10\text{-}20$ cm) (Not in table. 1).

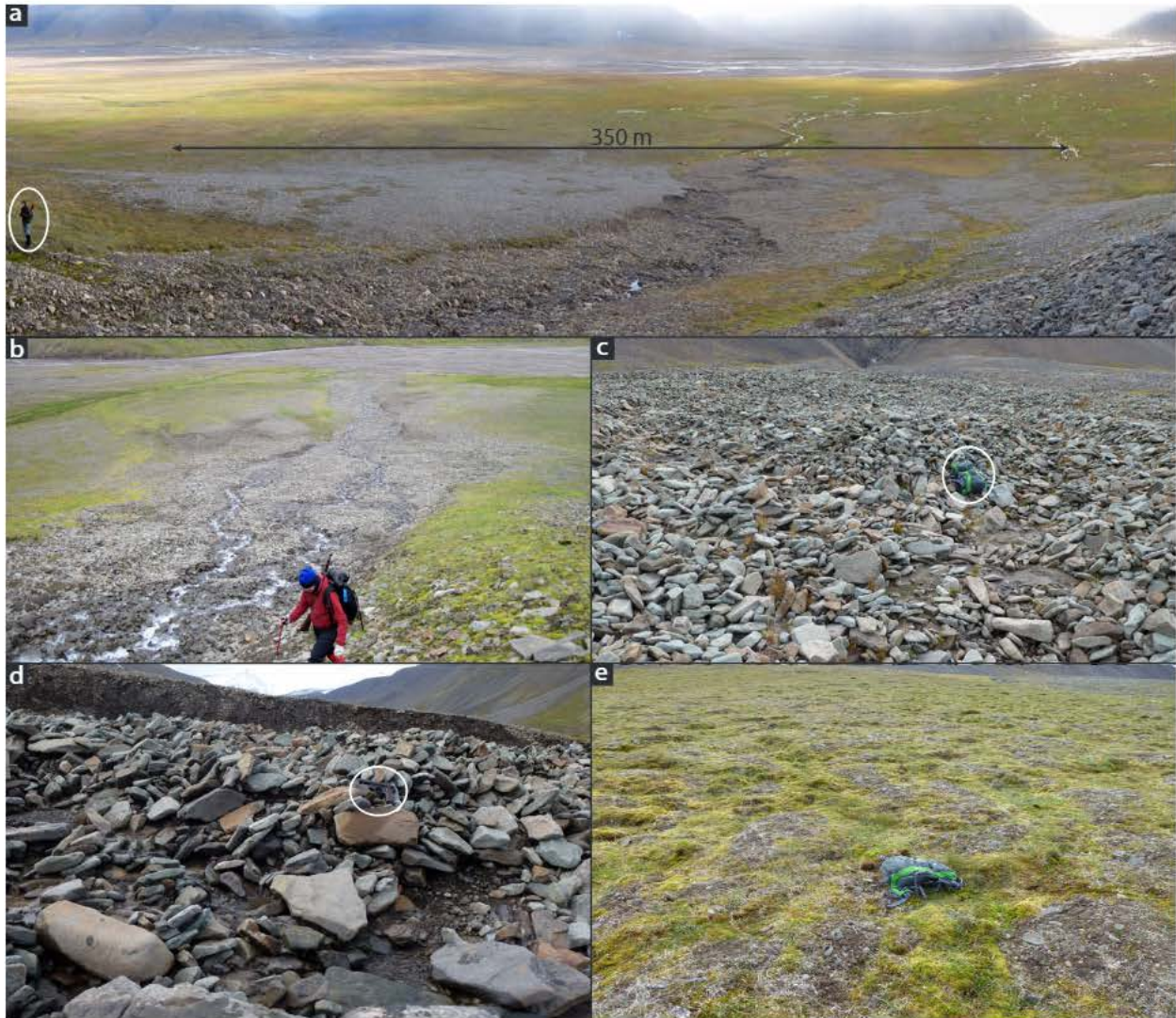


Figure 14: Fluvial-flow-dominated fans. (a) Fluvial-flow-dominated fan in Adventdalen (fan 38). (b) Fluvial-flow-dominated fan in Bjørndalen (fan 58). These fans are generally incised, separating the active part of the fan from the inactive part. The active part generally has typical braided planform due to the continuous discharge of meltwater in spring and summer. (c) Upfan view on the active part of fan 56. (d) Active part of fan 56, showing clast imbrication. Flare gun for scale. (e) Inactive fan surface of fan 57, the initial morphology is heavily modified and hummocks have formed (Fig. 15c,d).

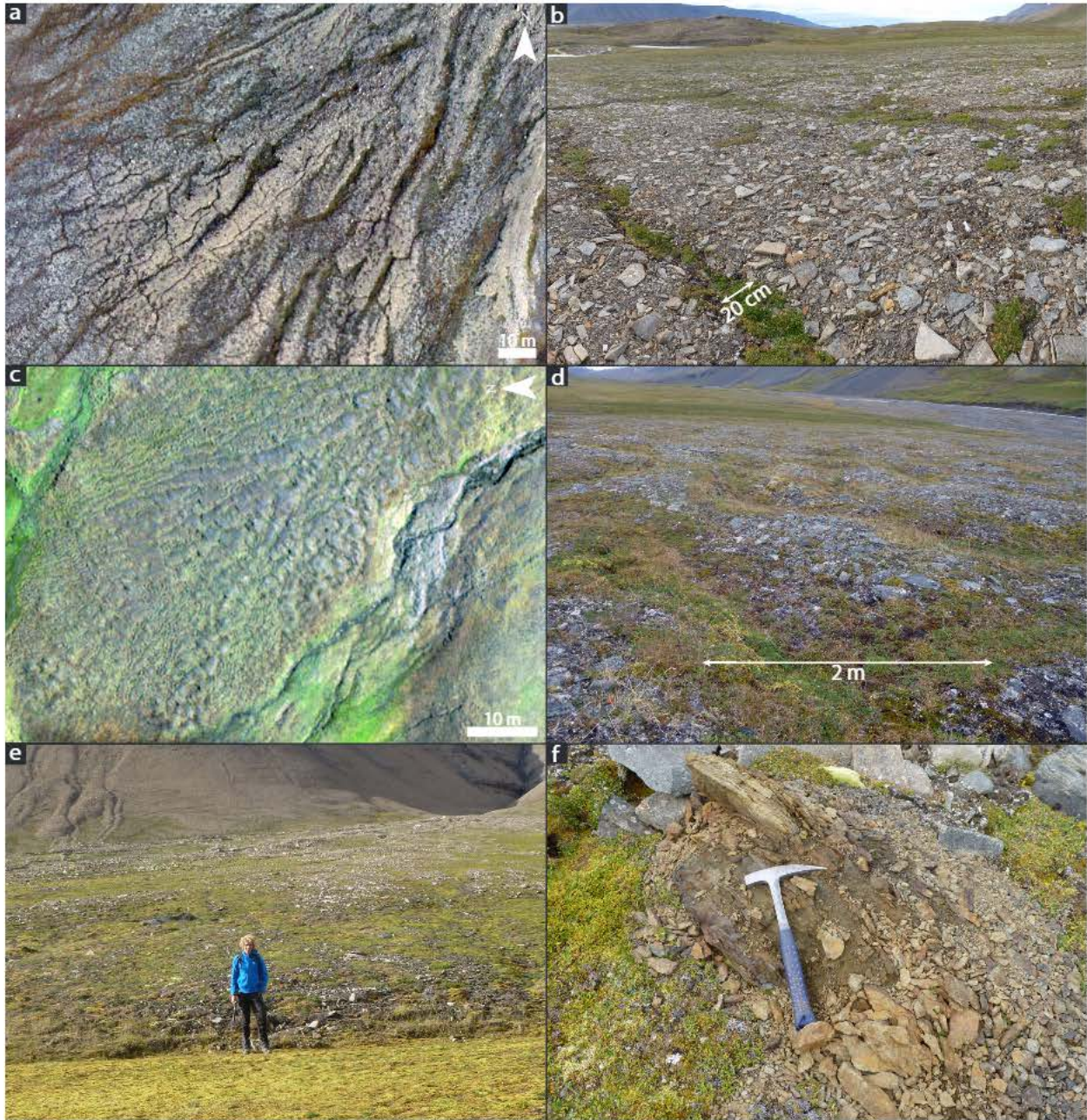


Figure 15: Morphology of inactive fan surfaces. (a) Polygonal ground on inactive fan surface of debris-flow-dominated fan in Adventdalen (fan 37). (b) Ground picture of polygonal ground shown in picture a. (c) Hummocks on inactive fan surface of a fluvial-flow-dominated fan in Bjørndalen (fan 57). (d) Ground picture of hummocks in picture c. (e) Stepped profile formed by solifluction at the foot of the inactive surface of fan 30 in Mälardalen. (f) Heavily fractured cobble by frost-weathering on fan 31 in Mälardalen.

512 5. Discussion

513 5.1. *Unique morphology and morphometry of fans in periglacial environments*

514 Our results show that perennial snowfall, recurrent snow avalanches, continuous per-
515 mafrost and frequent freeze-thaw cycles result in a unique morphology of fans on Svalbard.
516 This is in contrast with previous studies that suggested that processes leading to alluvial-fan
517 deposits differ little between different environments (e.g., Brierley et al., 1993; Harris and
518 Gustafson, 1993; Ibbeken et al., 1998; Webb and Fielding, 1999; Krzyszkowski and Zieliński,
519 2002; Harvey et al., 2005; Lafortune et al., 2006). The surface morphology and texture of
520 the studied colluvial fans are dominated by snow avalanches, in contrast to the rockfall-
521 dominated morphology and texture of colluvial fans in other regions. Snow avalanches can
522 also contribute sediment to and modify the primary morphology of debris-flow and fluvial-
523 flow-dominated alluvial fans. The inactive surfaces of these alluvial fans are be rapidly bev-
524 elled and levelled. Mainly by snow avalanches, but also by solifluction and frost weathering.
525 Periglacial reworking, such as the formation of ice-wedge polygons and hummocks, further
526 modifies these inactive surfaces. Below we elaborate on the uniqueness of the morphology
527 and texture of fans in the periglacial environment of Svalbard.

528 In general, the morphology of individual fluvial or debris-flow deposits on fans on Sval-
529 bard is similar to the morphology of these deposits in other environments, as found by Catto
530 (1993), Harris and Gustafson (1993) and Webb and Fielding (1999). However, debris-flow
531 size is often restricted by active-layer depth (André, 1990). Additionally, during summer
532 months fluvial and especially debris flows are relatively more abundant on Svalbard and
533 many other periglacial regions compared to other climatic regions. Fan surfaces are com-
534 pletely frozen and covered by snow during winter, and therefore fan activity is limited to the
535 spring and summer months (Webb and Fielding, 1999). Consequently, geomorphic activity
536 is more intense during the melting season as snowmelt and rainfall concordantly provide
537 discharge to the fans, and fluvial and debris flows can be triggered by a combination of
538 thawing of snow and ground ice and intense or longlasting rainfall (Decaulne and Sæmunds-
539 son, 2007). Moreover, rainfall and/or snowmelt thresholds for debris-flow initiation are low
540 and debris flows are easily triggered because of the permafrost table acting as an aquiclude
541 (e.g., Caine, 1980; Larsson, 1982; Sattler et al., 2011), especially in fine-grained arctic soils
542 (e.g., Harris and Lewkowicz, 2000; Lewkowicz and Harris, 2005).

543 Snow avalanches can be an important depositional mechanism on fans in periglacial
544 (e.g., Blikra and Nemeč, 1998; Decaulne and Sæmundsson, 2006; Siewert et al., 2012; Eck-
545 erstorfer et al., 2013) and Alpine environments (e.g., Jomelli and Francou, 2000; Jomelli
546 and Bertran, 2001). On Svalbard, snow avalanches were found to be an important geomor-
547 phic agent on fans, resulting in morphology that significantly differs from the morphology
548 of fans in environments where snow avalanches are less abundant or absent. The snow
549 avalanche-dominated fans are formed below typical snow avalanches chutes, have a flattened
550 cross-profile and sometimes a distinct basal concavity. There is a marked downstream coars-
551 ening grain size (Fig. 8), but in contrast to rockfall-dominated colluvial fans, which generally
552 have a more openwork texture (e.g., Friend et al., 2000; Ventra et al., 2013), the voids on
553 the proximal domain are filled with fine sediments, as snow avalanche erosion continuously

554 exposes the deeper talus, and only the coarser-grained distal domain has an openwork tex-
555 ture. Small-scale morphological traits, such as perched cobbles and boulders, debris-horns,
556 debris-tails and arcuate alignments of coarse debris, exclusively formed by snow avalanches
557 are present on these fans. In the Adventdalen region on Svalbard, we only found snow
558 avalanche-dominated colluvial fan surfaces. Yet, such a strong snow avalanche influence on
559 colluvial fans is probably not representative for all periglacial environments, as the plateau
560 mountains and strong and continuous winds in the Adventdalen region favor the forma-
561 tion of cornices, and cornice-fall avalanches (Eckerstorfer et al., 2013). For example, snow
562 avalanches frequently occur in many high-latitude northern hemisphere mountains (e.g.,
563 Rapp, 1985; Luckman, 1992), but scarcely occur on Antarctica. The primary effect of snow
564 avalanches on fluvial and debris-flow-dominated fans is much smaller than on colluvial fans,
565 as snow avalanches are less frequent because of lower sloping catchments. However, snow
566 avalanches were also found to contribute sediment to these fans, mainly in form of slush
567 avalanches, and can consequently have a profound effect on the surface morphology.

568 The secondary processes causing post-depositional modification and their resulting mor-
569 phology in the periglacial environment of Svalbard differ from those in other environments,
570 and are mainly associated with snow avalanches, presence of permafrost and freeze-thaw
571 cycles. Frost weathering breaks down surficial clasts, but remnants of broken-down debris
572 are far less abundant than commonly observed on fans in arid to semi-arid environments
573 (e.g., De Haas et al., 2014). Because of snow avalanche erosion, solifluction and weather-
574 ing, primary morphological features, especially debris-flow lobes and levees, are generally
575 short-living landforms on inactive fan sectors on Svalbard. André (1990) and André (1995)
576 found that recurrent snow avalanches rapidly erode, bevel and level the debris-flow levees
577 and lobes on some fans, and consequently their life span can be as low as 30-40 years. In
578 contrast, on slopes without snow avalanche chutes above, deposits can be preserved much
579 longer, for several centuries and locally more than a millennium (André, 1990). Similarly,
580 debris-flow levees were almost completely levelled in a 20 year period due to snow avalanche
581 activity in the Cairngorm Mountains in Scotland (Luckman, 1992). The vulnerability of fans
582 to snow avalanche erosion is strongly influenced by the dominant wind direction, as leeward
583 slopes are much more prone to snow avalanches (André, 1995; Eckerstorfer and Christiansen,
584 2011b; Siewert et al., 2012; Eckerstorfer et al., 2013).

585 In addition to the extensive fan modification by snow avalanches, solifluction was found
586 to affect the fan surfaces, and on some fans extensive areas with hummocks and/or ice-
587 wedge polygons developed (Fig. 15). Similarly, hummocks also form on the inactive domain
588 of fans in the semi-arid periglacial climate of the Aklavik Range, Canada, with continuous
589 permafrost (Legget et al., 1966; Catto, 1993). However, Webb and Fielding (1999) found
590 that fans in Antarctica experienced only small amounts of post-depositional modification,
591 restricted to wind ablation and limited runoff. In contrast, in arid to semi-arid environments
592 inactive fan surfaces are commonly reworked into a very different morphology. Here, inactive
593 surfaces are often heavily modified by a combination of weathering (mainly salt weathering),
594 runoff and wind erosion (e.g., Wells et al., 1987; Blair and McPherson, 2009; De Haas et al.,
595 2014). These processes decrease the relief on the inactive fan surfaces and break down
596 surface sediments, ultimately resulting in smooth and homogeneous desert pavement (e.g.,

597 Al-Farraj and Harvey, 2000; Frankel and Dolan, 2007). Moreover, as post-depositional
598 smoothing of primary relief can occur within a few decades (André, 1990; Luckman, 1992),
599 post-depositional modification can be a much faster process in periglacial environments
600 than in arid to semi-arid environments, where this generally takes thousands to hundreds of
601 thousands years (Matmon et al., 2006; Frankel and Dolan, 2007).

602 On Svalbard, and in many other recently deglaciated periglacial regions, fluvial-flow-
603 dominated fans often have a large fanhead incision (Ryder, 1971; Owen and Sharma, 1998;
604 Lønne and Nemec, 2004), which is generally ascribed to a decrease in sediment supply
605 after an initial paraglacial increase since deglaciation of the valleys. However, although
606 this is a valid explanation for the large fanhead incision in these environments, fanhead
607 incisions are common in many other environments (e.g., Nicholas et al., 2009), as besides
608 changes in sediment supply, tectonic uplift (Alexander and Leeder, 1987), and autogenic
609 behavior (Nicholas et al., 2009; Van Dijk et al., 2012) can also cause fanhead incision.
610 Moreover, long-term climate changes could cause similar similar effects, especially when
611 affecting precipitation amounts.

612 The large-scale morphometry of fans in the periglacial environment of Svalbard differs
613 insignificantly from the morphometry of fans in various arid to semi-arid regions (Harvey,
614 2011) (Fig. 5). On a smaller scale, the cross-sectional architecture of the investigated collu-
615 vial fans on Svalbard differs from the cross-sectional architecture of colluvial fans in many
616 other environments (e.g., Blair and McPherson, 2009), by its flattened cross-profile caused by
617 frequent snow-avalanche erosion (Fig. 6b-c). Moreover, snow avalanche-dominated fans have
618 a larger difference in apex-zone angle compared to distal-zone angle, then rockfall-dominated
619 colluvial fans (Jomelli and Francou, 2000) (Fig. 6a).

620 The unique morphodynamics of fans in periglacial environments will probably also result
621 in a unique stratigraphy. Stratigraphy is mostly formed by surface morphodynamics that
622 cause net aggradation. This relation between sedimentary process and product means that
623 the processes that dominantly form a fan surface can also be expected to form the stratigra-
624 phy (e.g., Paola and Borgman, 1991; Van De Lageweg et al., 2013), if those processes do not
625 change over time. For lack of observations this remains speculative, but snow avalanches are
626 known to form unique stratigraphic deposits (Blikra and Selvik, 1998; Blikra and Nemec,
627 1998). Features that distinguish snow-avalanche deposits from those of fluvial flows, debris
628 flows, debris-fall and rockfall include uneven or discontinuous bed geometry, large clast sizes
629 compared to bed thicknesses, random clast fabric and predominantly openwork (matrix-free)
630 gravel texture (Blikra and Selvik, 1998).

631 *5.2. Future development of fans in periglacial environments*

632 Global warming effects will be profound in the arctic (e.g., Christiansen et al., 2010;
633 Fjørland et al., 2012). Svalbard is especially sensitive to atmospheric and oceanic changes,
634 due to its location at the northern margins of the warm North-Atlantic ocean current (e.g.,
635 Aagaard and Carmack, 1989). In the last decades, mean annual temperatures increased
636 by $\sim 1^\circ\text{C}$ per decade, whilst winter warming was even more dramatic with an increase of
637 $\sim 2\text{-}3^\circ\text{C}$ per decade (Fjørland et al., 2012). Mean annual precipitation has increased with
638 2-4% per decade (Fjørland et al., 2012). As a result, the temperature of the permafrost

639 surface increased by approximately $0.07^{\circ}\text{C yr}^{-1}$ in the last decades, with indications of
640 recent accelerated warming (Isaksen et al., 2007). Global Circulation Models predict a 4-
641 6°C warming and a 5% precipitation increase in Svalbard by 2100 in the SRES A1b emission
642 scenario (Benestad, 2005). This will result in warming of $\sim 4^{\circ}\text{C}$ in the near surface layers
643 (<10 m depth) and a dramatic increase in active-layer thickness (Etzelmüller et al., 2011).

644 Geomorphic activity on steep snow avalanche-dominated colluvial fans is mainly in-
645 fluenced by the dominant winter wind direction (Siewert et al., 2012; Eckerstorfer et al.,
646 2013; Christiansen et al., 2013), as this determines the favorable slopes for snow-cornice
647 accretion, and fills the mountain ravines and gullies with thick snowpacks that may later
648 obstruct runoff, causing slush avalanches (Blikra and Nemeč, 1998). Hence, an increase in
649 average temperature will not directly affect the colluvial fans on Svalbard, rather potential
650 climate-induced changes in precipitation amount and dominant winter wind direction will
651 adjust snow avalanche sedimentation. Changes in winter wind direction will probably lead
652 to changes in the location of areas with extensive snow avalanche sedimentation and thus
653 snow avalanche fans and rock glaciers (Eckerstorfer et al., 2013). As precipitation rates in
654 the arctic have roughly increased by 14% in the last century and greatest increases were
655 observed in autumn and winter (Førland et al., 2012), cornice formation and corresponding
656 snow avalanche erosion and sedimentation will probably increase, leading to higher geomor-
657 phic activity on the colluvial fans. Especially an increase in the number of days with high
658 amounts of precipitation in winter may lead to a higher snow-avalanche frequency (Laute
659 and Beylich, 2014), and wet snow avalanches most likely become more frequent when the
660 rain-on-snow events during the winter season increase (Kronholm et al., 2006; Laute and
661 Beylich, 2014). In general, the increase in active-layer depth on Svalbard during recent years,
662 and especially during the last decades is similar to observations in other periglacial regions
663 (e.g., Romanovsky et al., 2010; Smith et al., 2010; Christiansen et al., 2010). Rising air
664 temperatures in the arctic regions and anticipated deeper active layers, will cause thaw to
665 advance into ice-rich frozen ground that has not thawed for many decades, centuries or even
666 millennia (Isaksen et al., 2007; Christiansen and Humlum, 2008; Harris et al., 2009), thereby
667 increasing the amount of sediment available for transport due to loss of soil stabilizing ice
668 (e.g., Zimmermann and Haeberli, 1993; Bardou et al., 2011; Schoeneich et al., 2011) and
669 the probability of soil failure and debris-flow initiation by a reduction of soil shear strength
670 (Nater et al., 2008; Rist, 2008; Sattler et al., 2011; Harris et al., 2011). In consequence, there
671 will likely be a marked increase in both the rates of solifluction and the volume of annual
672 sediment transport due to an increase in debris-flow frequency on Svalbard (Matsuoka, 2001;
673 Åkerman, 2005; Harris et al., 2011). The anticipated increased precipitation frequency and
674 magnitude will further increase debris-flow frequency (Rebetez et al., 1997; Huscroft et al.,
675 2003). Additionally, an increase in active-layer thickness will increase debris-flow volume
676 (Rist, 2008; Clague et al., 2012), especially as André (1990) indicates that the size of debris
677 flows on Svalbard is currently limited by the active-layer depth. Thus, climatic change on
678 Svalbard is likely to increase the frequency and magnitude of geomorphic events on fans.
679 Moreover, ongoing deglaciation will expose an increasing amount of slopes yielding large
680 volumes of sediment ready for transport to hillslopes and alluvial fans (Mercier et al., 2009).
681 The increase of coarse sediment supply may have adverse effects on the rivers in the valleys

682 and the increase of fine sediment supply to the fjords and coastal waters may adversely affect
683 the marine ecosystem.

684 Although the above analysis focuses on the geomorphic effects of global warming on
685 Svalbard, we anticipate a similar response in other arctic, antarctic and periglacial environ-
686 ments. However, the exact geomorphic response is site-specific and depends on local climatic
687 response to global warming (e.g., Pavlova et al., 2014).

688 6. Conclusions

689 We studied the effects of periglacial conditions on the morphology of snow avalanche-
690 dominated colluvial fans, and debris-flow- and fluvial-flow-dominated fans on Svalbard on
691 the basis of new data and literature review. Both snow avalanches and rockfall contribute
692 significant amounts of debris to colluvial fans, but snow avalanches were found to domi-
693 nate surface morphology and morphometry of the investigated colluvial fans. These fans
694 have flattened cross-profiles and fine-grained proximal domains due to avalanche erosion,
695 whereas the distal domains primarily consist of cobbles and boulders with an openwork tex-
696 ture. On a smaller scale the extensive snow avalanche activity is testified by the presence
697 of perched cobbles and boulders and debris horns and tails. In a few cases, where loose
698 sediment and snow avalanches are abundant, tongue-shaped colluvial fans are formed. Snow
699 avalanche-dominated colluvial fans are absent in most other environments on Earth, where
700 they generally form by rockfall.

701 The large-scale morphometry (e.g., catchment and fan area and slope) of debris-flow- and
702 fluvial-flow-dominated alluvial fans on Svalbard is similar to those in most other environ-
703 ments on Earth. The primary deposits of debris flows and fluvial flows are largely similar to
704 those in other environments, but the interaction of these processes with periglacial processes
705 on the fans leads to a unique morphology. Snow avalanches contribute significant amounts of
706 sediment to debris-flow- and fluvial-flow-dominated fans and modify both morphology and
707 sediment size-sorting patterns. On these fans, snow avalanches often have enough erosive
708 power to bevel and level the primary relief and reduce the sediment size-sorting formed by
709 the debris flows and fluvial flows. Frost weathering and solifluction probably contribute to
710 smoothing of the fan morphology. On the longer term, ice wedge polygonal ground, hum-
711 mmocks and solifluction sheets and lobes form on inactive fan surfaces, removing the primary
712 relief.

713 The intense global warming in arctic regions will most likely enhance geomorphic activity
714 on alluvial fans in these regions, as permafrost degradation will probably enhance debris-
715 flow frequency and magnitude. On the other hand, activity on colluvial fans is most likely
716 mainly influenced by shifts in dominant winter wind direction and resulting snow avalanche
717 activity.

718 7. Acknowledgments

719 This work is part of the PhD research of TdH, supported by the Netherlands Or-
720 ganisation for Scientific Research (NWO) and the Netherlands Space Office (NSO) (grant

721 ALW_GO_PL17_2012 to MGK). We gratefully acknowledge the Norwegian Polar Institute
722 (NPI) for logistical support during fieldwork. Special thanks go to Jørn Dybdahl of NPI for
723 help with planning and logistics, including all boat transport to and from the field sites and
724 to other aids to our survival. We further acknowledge DLR for the use of the HRSC-AX
725 data and Kolibri Geo Services for the high-resolution aerial images of fans in Adventdalen.
726 Constructive comments by Christopher R. Fielding and one anonymous reviewer are grate-
727 fully acknowledged. The authors contributed in the following proportions to conception and
728 study design, data collection, analysis and conclusions, and manuscript preparation: TdH
729 (40, 30, 60, 80)%, MGK (30, 30, 20, 20)%, PEC (20, 30, 0, 0)%, LR (0, 0, 10, 0)%, EH (10,
730 10, 10, 0)%.

731 **References**

- 732 Aagaard, K., Carmack, E., 1989. The role of sea ice and other fresh water in the Arctic circulation. *Journal*
733 *of Geophysical Research: Oceans* (1978–2012) 94 (C10), 14485–14498.
- 734 Agisoft, 2011. Image-based 3D modelling. Available at: www.agisoft.ru.
- 735 Åkerman, H. J., 1984. Notes on talus morphology and processes in Spitsbergen. *Geografiska Annaler. Series*
736 *A. Physical Geography* 66 (4), 267–284.
- 737 Åkerman, H. J., 2005. Relations between slow slope processes and active-layer thickness 1972–2002, Kapp
738 Linné, Svalbard. *Norsk Geografisk Tidsskrift* 59 (2), 116–128.
- 739 Al-Farraj, A., Harvey, A. M., 2000. Desert pavement characteristics on wadi terrace and alluvial fan surfaces:
740 Wadi Al-Bih, U.A.E. and Oman. *Geomorphology* 35 (34), 279–297.
- 741 Alexander, J., Leeder, M. R., 1987. Recent Developments in Fluvial Sedimentology. Society of Economic
742 Paleontologists and Mineralogists Special Publication 39, Ch. Active tectonic control on alluvial archi-
743 tecture, pp. 234–252.
- 744 André, M.-F., 1986. Dating slope deposits and estimating rates of rock wall retreat in northwest Spitsbergen
745 by lichenometry. *Geografiska Annaler. Series A. Physical Geography* 68 (1/2), 65–75.
- 746 André, M.-F., 1990. Frequency of debris flows and slush avalanches in Spitsbergen: a tentative evaluation
747 from lichenometry. *Polish Polar Research* 11, 345–363.
- 748 André, M.-F., 1990. Geomorphic impact of spring avalanches in Northwest Spitsbergen (79 N). *Permafrost*
749 *and Periglacial Processes* 1 (2), 97–110.
- 750 André, M.-F., 1995. Holocene climate fluctuations and geomorphic impact of extreme events in Svalbard.
751 *Geografiska Annaler* 77 (4), 241–250.
- 752 André, M.-F., 1997. Holocene rockwall retreat in Svalbard: a triple-rate evolution. *Earth Surface Processes*
753 *and Landforms* 22 (5), 423–440.
- 754 André, M.-F., 2003. Do periglacial landscapes evolve under periglacial conditions? *Geomorphology* 52 (1),
755 149–164.
- 756 Ballantyne, C. K., 2002. Paraglacial geomorphology. *Quaternary Science Reviews* 21 (18), 1935–2017.
- 757 Bardou, E., Favre-Bulle, G., Ornstein, P., Rouiller, J. D., 2011. Influence of the connectivity with permafrost
758 of the debris-flow triggering in high-alpine environment. *Italian Journal of Engineering Geology and*
759 *Environment* 10, 13–21.
- 760 Benestad, R., 2005. Climate change scenarios for northern Europe from multi-model IPCC AR4 climate
761 simulations. *Geophysical Research Letters* 32 (17), L17704.
- 762 Bibus, E., 1975. Geomorphologische Untersuchungen zur Hang-und Talentwicklung im zentralen West-
763 Spitzbergen. *Polarforschung* 45 (2), 102–119.
- 764 Blair, T. C., 1999. Sedimentology of the debris-flow-dominated Warm Spring Canyon alluvial fan, Death
765 Valley, California. *Sedimentology* 46 (5), 941–965.
- 766 Blair, T. C., McPherson, J. G., 1994. Alluvial fans and their natural distinction from rivers based on
767 morphology, hydraulic processes, sedimentary processes, and facies assemblages. *Journal of Sedimentary*
768 *Research* 64A, 450–489.
- 769 Blair, T. C., McPherson, J. G., 2009. Processes and forms of alluvial fans. In: Parsons, A., Abrahams, A.
770 (Eds.), *Geomorphology of Desert Environments*. Springer Netherlands, pp. 413–467.
- 771 Blikra, L. H., Nemeč, W., 1998. Postglacial colluvium in western Norway: depositional processes, facies and
772 palaeoclimatic record. *Sedimentology* 45 (5), 909–960.
- 773 Blikra, L. H., Selvik, S. F., 1998. Climatic signals recorded in snow avalanche-dominated colluvium in
774 western Norway: depositional facies successions and pollen records. *The Holocene* 8 (6), 631–658.
- 775 Bogen, J., Bønsnes, T. E., 2003. Erosion and sediment transport in High Arctic rivers, Svalbard. *Polar*
776 *Research* 22 (2), 175–189.
- 777 Brazier, V., Whittington, G., Ballantyne, C. K., 1988. Holocene debris cone evolution in Glen Etive, Western
778 Grampian Highlands, Scotland. *Earth Surface Processes and Landforms* 13 (6), 525–531.
- 779 Brierley, G. J., Liu, K., Crook, K. A., 1993. Sedimentology of coarse-grained alluvial fans in the Markham
780 Valley, Papua New Guinea. *Sedimentary Geology* 86 (3), 297–324.

- 781 Brown, J., Ferrians, O. J., Heginbottom, J., Melnikov, E., 1997. Circum-Arctic map of permafrost and
782 ground-ice conditions. US Geological Survey Map CP-45, Circum-Pacific Map Series, scale 1:10,000,000.
- 783 Bryant, I. D., 1982. Loess deposits in lower Adventdalen, Spitsbergen. *Polar Research* 1982 (2), 93–103.
- 784 Caine, N., 1980. The rainfall intensity-duration control of shallow landslides and debris flows. *Geografiska*
785 *Annaler A* 62 (1-2), 23–27.
- 786 Carbonneau, P. E., 2005. The threshold effect of image resolution on image-based automated grain size
787 mapping in fluvial environments. *Earth Surface Processes and Landforms* 30 (13), 1687–1693.
- 788 Carbonneau, P. E., Lane, S. N., Bergeron, N. E., 2004. Catchment-scale mapping of surface grain size in
789 gravel bed rivers using airborne digital imagery. *Water Resources Research* 40 (7), W07202.
- 790 Catto, N. R., 1993. Morphology and development of an alluvial fan in a permafrost region, Aklavik Range,
791 Canada. *Geografiska Annaler. Series A. Physical Geography* 75(3), 83–93.
- 792 Cavalli, M., Marchi, L., et al., 2008. Characterisation of the surface morphology of an alpine alluvial fan
793 using airborne LiDAR. *Natural Hazards and Earth System Science* 8 (2), 323–333.
- 794 Chiverrell, R., Harvey, A., Foster, G., 2007. Hillslope gullying in the Solway Firth-Morecambe Bay region,
795 Great Britain: Responses to human impact and/or climatic deterioration? *Geomorphology* 84 (3), 317–
796 343.
- 797 Christiansen, H. H., Etzelmüller, B., Isaksen, K., Juliussen, H., Farbrot, H., Humlum, O., Johansson, M.,
798 Ingeman-Nielsen, T., Kristensen, L., Hjort, J., et al., 2010. The thermal state of permafrost in the Nordic
799 area during the International Polar Year 2007–2009. *Permafrost and Periglacial Processes* 21 (2), 156–181.
- 800 Christiansen, H. H., Humlum, O., Eckerstorfer, M., 2013. Central Svalbard 2000-2011 meteorological dy-
801 namics and periglacial landscape response. *Arctic, Antarctic, and Alpine Research* 45 (1), 6–18.
- 802 Clague, J. J., Huggel, C., Korup, O., McGuire, B., 2012. Climate change and hazardous processes in high
803 mountains. *Revista de la Asociación Geológica Argentina* 69 (3), 328–338.
- 804 Dallmann, W., Kjærnet, T., Nøttvedt, A., 2001. Geomorphological and Quaternary Map of Svalbard. Norsk
805 Polarinstitutt Temakart 31/32, scale 1:100.000.
- 806 Dallmann, W., Ohta, Y., Elvevold, S., 2002. Bedrock Map of Svalbard and Jan Mayen. Norsk Polarinstitutt
807 Temakart 33, scale 1:750000.
- 808 Davies, T. R., Smart, C. C., Turnbull, J. M., 2003. Water and sediment outbursts from advanced Franz
809 Josef glacier, New Zealand. *Earth Surface Processes and Landforms* 28 (10), 1081–1096.
- 810 De Haas, T., Hauber, E., Kleinhans, M. G., 2013. Local late Amazonian boulder breakdown and denudation
811 rate on Mars. *Geophysical Research Letters* 40, 35273531.
- 812 De Haas, T., Ventra, D., Carbonneau, P. E., Kleinhans, M. G., 2014. Debris-flow dominance of alluvial fans
813 masked by runoff reworking and weathering. *Geomorphology* 217, 165–181.
- 814 Decaulne, A., Sæmundsson, T., 2003. Debris-flow characteristics in the Gleidarhjalli area, northwestern
815 Iceland. *Debris-flow hazards mitigation: mechanics, prediction, and assessment 2*, 1107–1118.
- 816 Decaulne, A., Sæmundsson, T., 2006. Geomorphic evidence for present-day snow-avalanche and debris-flow
817 impact in the Icelandic Westfjords. *Geomorphology* 80 (1), 80–93.
- 818 Decaulne, A., Sæmundsson, T., 2007. Spatial and temporal diversity for debris-flow meteorological control
819 in subarctic oceanic periglacial environments in Iceland. *Earth Surface Processes and Landforms* 32 (13),
820 1971–1983.
- 821 Derbyshire, E., Owen, L. A., 1990. Quaternary alluvial fans in the Karakoram Mountains. *Alluvial Fans: A*
822 *Field Approach*. Wiley, Chichester, 27–53.
- 823 Dorn, R. I., 1994. The role of climatic change in alluvial fan development. In: *Geomorphology of Desert*
824 *Environments*. Springer, pp. 593–615.
- 825 Eckerstorfer, M., Christiansen, H. H., 2011a. The “High Arctic Maritime Snow Climate” in Central Svalbard.
826 *Arctic, Antarctic, and Alpine Research* 43 (1), 11–21.
- 827 Eckerstorfer, M., Christiansen, H. H., 2011b. Topographical and meteorological control on snow avalanching
828 in the Longyearbyen area, central Svalbard 2006–2009. *Geomorphology* 134 (3), 186–196.
- 829 Eckerstorfer, M., Christiansen, H. H., 2012. Meteorology, topography and snowpack conditions causing two
830 extreme mid-winter slush and wet slab avalanche periods in high arctic maritime Svalbard. *Permafrost*
831 *and Periglacial Processes* 23 (1), 15–25.

- 832 Eckerstorfer, M., Christiansen, H. H., Rubensdotter, L., Vogel, S., 2013. The geomorphological effect of
833 cornice fall avalanches in the Longyeardalen valley, Svalbard. *The Cryosphere* 7 (5), 1361–1374.
- 834 Eckerstorfer, M., Christiansen, H. H., Vogel, S., Rubensdotter, L., 2012. Snow cornice dynamics as a control
835 on plateau edge erosion in central Svalbard. *Earth Surface Processes and Landforms* 38(5), 466–476.
- 836 Etzelmüller, B., Schuler, T., Isaksen, K., Christiansen, H., Farbro, H., Benestad, R., 2011. Modeling the
837 temperature evolution of Svalbard permafrost during the 20th and 21st century. *The Cryosphere* 5 (1),
838 67–79.
- 839 Eyles, N., Kocsis, S., 1988. Sedimentology and clast fabric of subaerial debris flow facies in a glacially-
840 influenced alluvial fan. *Sedimentary Geology* 59 (1), 15–28.
- 841 Fonstad, M. A., Dietrich, J. T., Courville, B. C., Jensen, J. L., Carbonneau, P. E., 2013. Topographic
842 structure from motion: a new development in photogrammetric measurement. *Earth Surface Processes
843 and Landforms* 38 (4), 421–430.
- 844 Førland, E., Hanssen-Bauer, I., Nordli, P., 1997. Climate statistics and longterm series of temperature and
845 precipitation at Svalbard and Jan Mayen. *Norwegian Meteorological Institute Report*, 21/97.
- 846 Førland, E. J., Benestad, R., Hanssen-Bauer, I., Haugen, J. E., Skaugen, T. E., 2012. Temperature and
847 precipitation development at Svalbard 1900–2100. *Advances in Meteorology* 2011.
- 848 Førland, E. J., Hanssen-Bauer, I., 2003. Past and future climate variations in the Norwegian Arctic: overview
849 and novel analyses. *Polar Research* 22 (2), 113–124.
- 850 Frankel, K. L., Dolan, J. F., 2007. Characterizing arid region alluvial fan surface roughness with airborne
851 laser swath mapping digital topographic data. *J. Geophys. Res.* 112 (F2), F02025.
- 852 Friend, D. A., Phillips, F. M., Campbell, S. W., Liu, T., Sharma, P., 2000. Evolution of desert colluvial
853 boulder slopes. *Geomorphology* 36 (1), 19–45.
- 854 Frings, R. M., 2008. Downstream fining in large sand-bed rivers. *Earth-Science Reviews* 87 (1), 39–60.
- 855 Gwinner, K., Hauber, E., Jaumann, R., Neukum, G., 2000. High-resolution, digital photogrammetric map-
856 ping: A tool for Earth science. *Eos, Transactions American Geophysical Union* 81 (44), 513–520.
- 857 Hanssen-Bauer, I., Førland, E., 1998. Long-term trends in precipitation and temperature in the Norwegian
858 Arctic: can they be explained by changes in atmospheric circulation patterns? *Climate Research* 10 (2),
859 143–153.
- 860 Harris, C., Kern-Luetsch, M., Christiansen, H. H., Smith, F., 2011. The role of interannual climate variabil-
861 ity in controlling solifluction processes, Endalen, Svalbard. *Permafrost and Periglacial Processes* 22 (3),
862 239–253.
- 863 Harris, C., Lewkowicz, A. G., 2000. An analysis of the stability of thawing slopes, Ellesmere Island, Nunavut,
864 Canada. *Canadian Geotechnical Journal* 37 (2), 449–462.
- 865 Harris, S., McDermid, G., 1998. Frequency of debris flows on the Sheep Mountain fan, Kluane Lake, Yukon
866 Territory. *Zeitschrift für Geomorphologie* 42 (2), 159–175.
- 867 Harris, S. A., Gustafson, C. A., 1993. Debris flow characteristics in an area of continuous permafrost, St.
868 Elias Range, Yukon Territory. *Zeitschrift für Geomorphologie* 37, 41–41.
- 869 Hartley, A. J., Mather, A. E., Jolley, E., Turner, P., 2005. Alluvial Fans: Geomorphology, Sedimentology,
870 Dynamics. Geological Society London Special Publication, Ch. Climatic controls on alluvial-fan activity,
871 Coastal Cordillera, northern Chile, pp. 95–115.
- 872 Hartley, A. J., Weissmann, G. S., Nichols, G. J., Warwick, G. L., 2010. Large distributive fluvial systems:
873 characteristics, distribution, and controls on development. *Journal of Sedimentary Research* 80 (2), 167–
874 183.
- 875 Harvey, A., 2011. Dryland alluvial fans. *Arid Zone Geomorphology: Process, Form and Change in Drylands*,
876 Third Edition, 333–371.
- 877 Harvey, A. M., 2010. Sediment Cascades: An integrated approach. John Wiley & Sons, Ltd, Ch. Local
878 Buffers to the Sediment Cascade: Debris Cones and Alluvial Fans, pp. 153–180.
- 879 Harvey, A. M., Mather, A. E., Stokes, M., 2005. Alluvial fans: geomorphology, sedimentology, dynamics -
880 introduction. a review of alluvial-fan research. Geological Society, London, Special Publications 251 (1),
881 1–7.
- 882 Hauber, E., Platz, T., Reiss, D., Le Deit, L., Kleinhans, M. G., Marra, W. A., de Haas, T., Carbonneau,

- 883 P., 2013. Asynchronous formation of Hesperian and Amazonian-aged deltas on Mars and implications for
884 climate. *Journal of Geophysical Research: Planets* 118 (7), 1529–1544.
- 885 Hauber, E., Reiss, D., Ulrich, M., Preusker, F., Trauthan, F., Zanetti, M., Hiesinger, H., Jaumann, R.,
886 Johansson, L., Johnsson, A., O. M. C. E. J. H. M. S., 2011. Landscape evolution in Martian mid-latitude
887 regions: insights from analogous periglacial landforms in Svalbard. *Geological Society, London, Special
888 Publications* 356 (1), 111–131.
- 889 Hestnes, E., 1998. Slushflow hazard—where, why and when? 25 years of experience with slushflow consulting
890 and research. *Annals of Glaciology* 26, 370–376.
- 891 Humlum, O., Christiansen, H. H., Juliussen, H., 2007. Avalanche-derived rock glaciers in Svalbard. *Perma-
892 frost and Periglacial Processes* 18 (1), 75–88.
- 893 Huscroft, C. A., Lipovsky, P., Bond, J. D., 2003. Permafrost and landslide activity: Case studies from
894 southwestern Yukon Territory. *Yukon Geological Survey*, pp. 107–119.
- 895 Ibbeken, H., Warnke, D. A., Diepenbroek, M., 1998. Granulometric study of the Hanaupah Fan, Death
896 Valley, California. *Earth Surface Processes and Landforms* 23 (6), 481–492.
- 897 Isaksen, K., Holmlund, P., Sollid, J. L., Harris, C., 2001. Three deep Alpine-permafrost boreholes in Svalbard
898 and Scandinavia. *Permafrost and Periglacial Processes* 12 (1), 13–25.
- 899 Isaksen, K., Mühl, D. V., Gubler, H., Kohl, T., Sollid, J. L., 2000. Ground surface-temperature reconstruc-
900 tion based on data from a deep borehole in permafrost at Janssonhaugen, Svalbard. *Annals of Glaciology*
901 31 (1), 287–294.
- 902 Isaksen, K., Sollid, J. L., Holmlund, P., Harris, C., 2007. Recent warming of mountain permafrost in Svalbard
903 and Scandinavia. *Journal of Geophysical Research: Earth Surface* (2003–2012) 112 (F2), F02S04.
- 904 Jahn, A., 1967. Some features of mass movement on Spitsbergen slopes. *Geografiska Annaler. Series A.
905 Physical Geography* 49, 213–225.
- 906 Jahn, A., 1976. Contemporaneous geomorphological processes in Longyeardalen, Vest-Spitsbergen (Sval-
907 bard). *Biuletyn Peryglacjalny* 26, 253–268.
- 908 Jamieson, J. B., Schweizer, J., 2000. Texture and strength changes of buried surface-hoar layers with impli-
909 cations for dry snow-slab avalanche release. *Journal of Glaciology* 46 (152), 151–160.
- 910 Jaumann, R., Neukum, G., Behnke, T., Duxbury, T., Eichentopf, K., Flohrer, J., Gasselt, S., Giese, B.,
911 Gwinner, K., Hauber, E., Hoffmann, H., Hoffmeister, A., Köhler, U., Matz, K.-D., McCord, T., Mertens,
912 V., Oberst, J., Pischel, R., Reiss, D., Ress, E., Roatsch, T., Saiger, P., Scholten, F., Schwarz, G.,
913 Stephan, K., Wählisch, M., 2007. The high-resolution stereo camera (HRSC) experiment on Mars Express:
914 Instrument aspects and experiment conduct from interplanetary cruise through the nominal mission.
915 *Planetary and Space Science* 55 (7), 928–952.
- 916 Jóhannesson, T., Arnalds, T., 2001. Accidents and economic damage due to snow avalanches and landslides
917 in Iceland. *Jökull* 50, 81–94.
- 918 Johnsson, A., Reiss, D., Hauber, E., Zanetti, M., Hiesinger, H., Johansson, L., Olvmo, M., 2012. Periglacial
919 mass-wasting landforms on Mars suggestive of transient liquid water in the recent past: Insights from
920 solifluction lobes on Svalbard. *Icarus* 218 (1), 489–505.
- 921 Jomelli, V., Bertran, P., 2001. Wet snow avalanche deposits in the French Alps: structure and sedimentology.
922 *Geografiska Annaler: series A, physical geography* 83 (1-2), 15–28.
- 923 Jomelli, V., Francou, B., 2000. Comparing the characteristics of rockfall talus and snow avalanche land-
924 forms in an Alpine environment using a new methodological approach: Massif des Ecrins, French Alps.
925 *Geomorphology* 35 (3), 181–192.
- 926 Kesel, R., Spicer, B., 1985. Geomorphologic relationships and ages of soils on alluvial fans in the Rio General
927 valley, Costa Rica. *Catena* 12 (1), 149–166.
- 928 Kostaschuk, R., MacDonald, G., Putnam, P., 1986. Depositional process and alluvial fan-drainage basin
929 morphometric relationships near Banff, Alberta, Canada. *Earth Surface Processes and Landforms* 11 (5),
930 471–484.
- 931 Kronholm, K., Vikhamar-Schuler, D., Jaedicke, C., Isaksen, K., Sorteberg, A., Kristensen, K., 2006. Fore-
932 casting snow avalanche days from meteorological data using classification trees; Grasdalen, Western Nor-
933 way. In: *Proceedings of the International Snow Science Workshop, Telluride, Colorado*. pp. 1–6.

- 934 Krzyszkowski, D., Zieliński, T., 2002. The Pleistocene end moraine fans: controls on their sedimentation
935 and location. *Sedimentary Geology* 149 (1), 73–92.
- 936 Lafortune, V., Filion, L., Héту, B., 2006. Impacts of Holocene climatic variations on alluvial fan activity
937 below snowpatches in subarctic Québec. *Geomorphology* 76 (3), 375–391.
- 938 Larsson, S., 1982. Geomorphological effects on the slopes of Longyear valley, Spitsbergen, after a heavy
939 rainstorm in July 1972. *Geografiska Annaler. Series A. Physical Geography* 64, 105–125.
- 940 Latham, J., Montagne, J., 1970. The possible importance of electrical forces in the development of snow
941 cornices. *Journal of Glaciology* 9, 375–384.
- 942 Laute, K., Beylich, A. A., 2014. Morphometric and meteorological controls on recent snow avalanche dis-
943 tribution and activity at hillslopes in steep mountain valleys in western Norway. *Geomorphology* 218,
944 16–34.
- 945 Legget, R. F., Brown, R. E., Johnston, G. H., 1966. Alluvial fan formation near Aklavik, Northwest Terri-
946 tories, Canada. *Geological Society of America Bulletin* 77 (1), 15–30.
- 947 Lewkowicz, A. G., Harris, C., 2005. Morphology and geotechnique of active-layer detachment failures in
948 discontinuous and continuous permafrost, northern Canada. *Geomorphology* 69 (1), 275–297.
- 949 Liestøl, O., 1976. Pingos, springs and permafrost in Spitsbergen. In: *Norsk Polarinstitutt Årbok 1975*. pp.
950 7–29.
- 951 Lønne, I., Nemeč, W., 2004. High-arctic fan delta recording deglaciation and environment disequilibrium.
952 *Sedimentology* 51 (3), 553–589.
- 953 Lorenz, R. D., Lopes, R. M., Paganelli, F., Lunine, J. I., Kirk, R. L., Mitchell, K. L., Soderblom, L. A.,
954 Stofan, E. R., Ori, G., Myers, M., et al., 2008. Fluvial channels on Titan: initial Cassini RADAR
955 observations. *Planetary and Space Science* 56 (8), 1132–1144.
- 956 Luckman, B., 1977. The geomorphic activity of snow avalanches. *Geografiska Annaler. Series A. Physical*
957 *Geography*, 31–48.
- 958 Luckman, B., 1992. Debris flows and snow avalanche landforms in the Lairig Ghru, Cairngorm Mountains,
959 Scotland. *Geografiska Annaler. Series A. Physical Geography* 74, 109–121.
- 960 Major, H., N. J., 1972. *Geology of the Adventdalen Map Area*. Norsk Polarinstitutt Skrifter 138.
- 961 Mangerud, J., Bolstad, M., Elgersma, A., Helliksen, D., Landvik, J. Y., Lønne, I., Lycke, A. K., Salvigsen,
962 O., Sandahl, T., Svendsen, J. I., 1992. The last glacial maximum on Spitsbergen, Svalbard. *Quaternary*
963 *Research* 38 (1), 1–31.
- 964 Matmon, A., Nichols, K., Finkel, R., 2006. Isotopic insights into smoothening of abandoned fan surfaces,
965 Southern California. *Quaternary Research* 66 (1), 109–118.
- 966 Matsuoka, N., 1991. A model of the rate of frost shattering: application to field data from Japan, Svalbard
967 and Antarctica. *Permafrost and Periglacial Processes* 2 (4), 271–281.
- 968 Matsuoka, N., 2001. Solifluction rates, processes and landforms: a global review. *Earth-Science Reviews*
969 55 (1), 107–134.
- 970 Matsuoka, N., Hirakawa, K., 2000. Solifluction resulting from one-sided and two-sided freezing: field data
971 from Svalbard. *Polar Geoscience* 13, 187–201.
- 972 Mercier, D., Étienne, S., Sellier, D., André, M.-F., 2009. Paraglacial gullying of sediment-mantled slopes:
973 a case study of Colletthøgda, Kongsfjorden area, West Spitsbergen (Svalbard). *Earth Surface Processes*
974 *and Landforms* 34 (13), 1772–1789.
- 975 Moscariello, A., Marchi, L., Maraga, F., Mortara, G., 2002. Alluvial fans in the Italian Alps: sedimentary
976 facies and processes. *Flood and Megaflood Processes and Deposits: Recent and Ancient Examples (Special*
977 *Publication 32 of the IAS)* 32, 141–166.
- 978 Nater, P., Arenson, L. U., Springman, S. M., 2008. Choosing geotechnical parameters for slope stability
979 assessments in alpine permafrost soils. In: *Ninth International Conference on Permafrost*, University of
980 Alaska Fairbanks. Vol. 29. pp. 1261–1266.
- 981 Nemeč, W., Postma, G., 1993. *Alluvial Sedimentation*. Blackwell Publishing Ltd., Oxford, UK, Ch. Quater-
982 nary alluvial fans in southwestern Crete: sedimentation processes and geomorphic evolution, pp. 235–276.
- 983 Nesje, A., Bakke, J., Dahl, S. O., Lie, Ø., Bøe, A.-G., 2007. A continuous, high-resolution 8500-yr snow-
984 avalanche record from western Norway. *The Holocene* 17 (2), 269–277.

- 985 Neukum, G., the HRSC-Team, 2001. The Airborne HRSC-AX cameras: evaluation of the technical concept
986 and presentation of application results after one year of operations. In: *Photogrammetric Week*. Vol. 1.
987 pp. 117–130.
- 988 Nicholas, A., Clarke, L., Quine, T., 2009. A numerical modelling and experimental study of flow width
989 dynamics on alluvial fans. *Earth Surface Processes and Landforms* 34 (15), 1985–1993.
- 990 Nyberg, R., 1989. Observations of slushflows and their geomorphological effects in the Swedish mountain
991 area. *Geografiska Annaler* 71A (3-4) 71, 185–198.
- 992 Owen, L. A., Sharma, M. C., 1998. Rates and magnitudes of paraglacial fan formation in the Garhwal
993 Himalaya: implications for landscape evolution. *Geomorphology* 26 (1), 171–184.
- 994 Paola, C., Borgman, L., 1991. Reconstructing random topography from preserved stratification. *Sedimen-*
995 *tology* 38 (4), 553–565.
- 996 Parker, J. R., 1967. The Jurassic and Cretaceous sequence in Spitsbergen. *Geological Magazine* 104 (5),
997 487–505.
- 998 Pavlova, I., Jomelli, V., Brunstein, D., Grancher, D., Martin, E., Déqué, M., 2014. Debris flow activity
999 related to recent climate conditions in the French Alps: a regional investigation. *Geomorphology* 219,
1000 248–259.
- 1001 Rachlewicz, G., 2010. Paraglacial modifications of glacial sediments over millennial to decadal time-scales
1002 in the high Arctic (Billefjorden, central Spitsbergen, Svalbard). *Quaestiones Geographicae* 29 (3), 59–67.
- 1003 Rapp, A., 1960. Talus slopes and mountain walls at Tempelfjorden, Spitsbergen: a geomorphological study
1004 of the denudation of slopes in an arctic locality. *Norsk Polarinstitutts Skrifter* 119, 1–96.
- 1005 Rapp, A., 1985. Extreme rainfall and rapid snowmelt as causes of mass movements in high latitude moun-
1006 tains. *Field and Theory, Lectures Geocryology*, 36–56.
- 1007 Rapp, A., 1986. Slope processes in high latitude mountains. *Progress in physical geography* 10 (1), 53–68.
- 1008 Rebetz, M., Lugon, R., Baeriswyl, P.-A., 1997. Climatic change and debris flows in high mountain regions:
1009 the case study of the Ritigraben torrent (Swiss Alps). *Climatic change* 36 (3-4), 371–389.
- 1010 Reiss, D., Hauber, E., Hiesinger, H., Jaumann, R., Trauthan, F., Preusker, F., Zanetti, M., Ulrich, M.,
1011 Johnsson, A., Johansson, L., et al., 2011. Terrestrial gullies and debris-flow tracks on Svalbard as planetary
1012 analogs for Mars. *Geological Society of America Special Papers* 483, 165–175.
- 1013 Rist, A., 2008. Hydrothermal processes within the active layer above alpine permafrost in steep scree slopes
1014 and their influence on slope stability. Ph.D. thesis, Geograph. Inst. der Univ. Zürich.
- 1015 Ritter, J. B., Miller, J. R., Enzel, Y., Wells, S. G., 1995. Reconciling the roles of tectonism and climate in
1016 Quaternary alluvial fan evolution. *Geology* 23 (3), 245–248.
- 1017 Romanovsky, V., Drozdov, D., Oberman, N., Malkova, G., Kholodov, A., Marchenko, S., Moskalenko, N.,
1018 Sergeev, D., Ukrainitseva, N., Abramov, A., et al., 2010. Thermal state of permafrost in Russia. *Permafrost*
1019 *and Periglacial Processes* 21 (2), 136–155.
- 1020 Roof, S., Werner, A., 2011. Indirect growth curves remain the best choice for lichenometry: evidence from
1021 directly measured growth rates from Svalbard. *Arctic, Antarctic, and Alpine Research* 43 (4), 621–631.
- 1022 Rozema, J., Boelen, P., Solheim, B., Zielke, M., Buskens, A., Doorenbosch, M., Fijn, R., Herder, J.,
1023 Callaghan, T., Björn, L. O., et al., 2006. Stratospheric ozone depletion: high arctic tundra plant growth
1024 on Svalbard is not affected by enhanced UV-B after 7 years of UV-B supplementation in the field. *Plant*
1025 *Ecology* 182 (1-2), 121–135.
- 1026 Ryder, J., 1971. The stratigraphy and morphology of para-glacial alluvial fans in south-central British
1027 Columbia. *Canadian Journal of Earth Sciences* 8 (2), 279–298.
- 1028 Saito, K., Oguchi, T., 2005. Slope of alluvial fans in humid regions of Japan, Taiwan and the Philippines.
1029 *Geomorphology* 70 (1), 147–162.
- 1030 Sattler, K., Keiler, M., Zischg, A., Schrott, L., 2011. On the connection between debris flow activity and
1031 permafrost degradation: a case study from the Schnalstal, South Tyrolean Alps, Italy. *Permafrost and*
1032 *Periglacial Processes* 22 (3), 254–265.
- 1033 Schoeneich, P., Dall’Amico, M., Deline, P., Zischg, A., 2011. Hazards related to permafrost and to permafrost
1034 degradation. PermaNET project, report 6.2. On-line publication ISBN 978-2-903095-59-8.
- 1035 Siewert, M. B., Krautblatter, M., Christiansen, H. H., Eckerstorfer, M., 2012. Arctic rockwall retreat rates

- 1036 estimated using laboratory-calibrated ERT measurements of talus cones in Longyeardalen, Svalbard.
1037 *Earth Surface Processes and Landforms* 37 (14), 1542–1555.
- 1038 Smith, S., Romanovsky, V., Lewkowicz, A., Burn, C., Allard, M., Clow, G., Yoshikawa, K., Throop, J.,
1039 2010. Thermal state of permafrost in North America: A contribution to the International Polar Year.
1040 *Permafrost and Periglacial Processes* 21 (2), 117–135.
- 1041 Sollid, J., Holmlund, P., Isaksen, K., Harris, C., 2000. Deep permafrost boreholes in western Svalbard,
1042 northern Sweden and southern Norway. *Norsk Geografisk Tidsskrift* 54 (4), 186–191.
- 1043 Sørbel, L., Tolgensbakk, J., 2002. Ice-wedge polygons and solifluction in the Adventdalen area, Spitsbergen,
1044 Svalbard. *Norsk Geografisk Tidsskrift* 56 (2), 62–66.
- 1045 Sørbel, L., Tolgensbakk, J., Hagen, J., Hogvard, K., 2011. Geomorphological and quaternary geological map
1046 of Svalbard, 1:100,000, C9G Adventdalen. *Norsk Polar Institutt Temakart* 31/32.
- 1047 Svendsen, J. I., Mangerud, J., 1997. Holocene glacial and climatic variations on Spitsbergen, Svalbard. *The*
1048 *Holocene* 7 (1), 45–57.
- 1049 Szpikowski, J., Szpikowska, G., Zwoliński, Z., Rachlewicz, G., Kostrzewski, A., Marciniak, M., Dragon,
1050 K., 2014. Character and rate of denudation in a High Arctic glacierized catchment (Ebbaelva, Central
1051 Spitsbergen). *Geomorphology* 218, 52–62.
- 1052 Thiedig, v. F., Kresling, A., 1973. Meteorologische und geologische Bedingungen bei der Entstehung von
1053 Muren im Juli 1972 auf Spitzbergen. *Polarforschung* 43 (1/2), 40–49.
- 1054 Van De Lageweg, W. I., Dijk, W. M., Kleinhans, M. G., 2013. Channel belt architecture formed by a
1055 meandering river. *Sedimentology* 60 (3), 840–859.
- 1056 Van Dijk, M., Kleinhans, M. G., Postma, G., Kraal, E., 2012. Contrasting morphodynamics in alluvial fans
1057 and fan deltas: effect of the downstream boundary. *Sedimentology* 59 (7), 2125–2145.
- 1058 Van Vliet-Lanoë, B., 1998. Frost and soils: implications for paleosols, paleoclimates and stratigraphy. *Catena*
1059 34 (1), 157–183.
- 1060 Ventra, D., Diaz, G. C., de Boer, P. I., 2013. Colluvial sedimentation in a hyperarid setting (Atacama
1061 Desert, northern Chile): Geomorphic controls and stratigraphic facies variability. *Sedimentology* 60 (5),
1062 1257–1290.
- 1063 Vogel, S., Eckerstorfer, M., Christiansen, H., 2012. Cornice dynamics and meteorological control at Gruvef-
1064 jellet, Central Svalbard. *The Cryosphere* 6 (1), 157–171.
- 1065 Webb, J., Fielding, C. R., 1999. Debris flow and sheetflood fans of the northern Prince Charles Mountains,
1066 East Antarctica. In: Miller, A. J., Gupta, A. (Eds.), *Varieties of Fluvial form*. Wiley, pp. 317–341.
- 1067 Weissmann, G., Hartley, A., Nichols, G., Scuderi, L., Olson, M., Buehler, H., Banteah, R., 2010. Fluvial
1068 form in modern continental sedimentary basins: Distributive fluvial systems. *Geology* 38 (1), 39–42.
- 1069 Wells, S. G., McFadden, L. D., Dohrenwend, J. C., 1987. Influence of late Quaternary climatic changes on
1070 geomorphic and pedogenic processes on a desert piedmont, Eastern Mojave Desert, California. *Quaternary*
1071 *Research* 27 (2), 130–146.
- 1072 Werner, A., 1990. Lichen growth rates for the northwest coast of Spitsbergen, Svalbard. *Arctic and Alpine*
1073 *Research* 22 (2), 129–140.
- 1074 Whipple, K. X., Dunne, T., 1992. The influence of debris-flow rheology on fan morphology, Owens Valley,
1075 California. *Geological Society of America Bulletin* 104 (7), 887–900.
- 1076 Zimmermann, M., Haeberli, W., 1993. Climatic change and debris flow activity in high-mountain areas—a
1077 case study in the Swiss Alps. *Catena Supplement* 22, 59–59.

